

1 **Ice Giant Systems: The Scientific Potential of Missions to Uranus and Neptune**

2

3 **Leigh N. Fletcher** (School of Physics and Astronomy, University of Leicester, University Road, Leicester, LE1
4 7RH, UK; leigh.fletcher@le.ac.uk; Tel: +441162523585), **Ravit Helled** (University of Zurich, Switzerland), **Elias
5 Roussos** (Max Planck Institute for Solar System Research, Germany), **Geraint Jones** (Mullard Space Science
6 Laboratory, UK), **Sébastien Charnoz** (Institut de Physique du Globe de Paris, France), **Nicolas André** (Institut
7 de Recherche en Astrophysique et Planétologie, Toulouse, France), **David Andrews** (Swedish Institute of
8 Space Physics, Sweden), **Michele Bannister** (Queens University Belfast, UK), **Emma Bunce** (University of
9 Leicester, UK), **Thibault Cavalié** (Université de Bordeaux, France), **Francesca Ferri** (Università degli Studi di
10 Padova, Italy), **Jonathan Fortney** (University of Santa-Cruz, USA), **Davide Grassi** (Istituto Nazionale di
11 AstroFisica – Istituto di Astrofisica e Planetologia Spaziali (INAF-IAPS), Rome, Italy), **Léa Griton** (Institut de
12 Recherche en Astrophysique et Planétologie, CNRS, Toulouse, France), **Paul Hartogh** (Max-Planck-Institut für
13 Sonnensystemforschung, Germany), **Ricardo Hueso** (Escuela de Ingeniería de Bilbao, UPV/EHU, Bilbao,
14 Spain), **Yohai Kaspi** (Weizmann Institute of Science, Israel), **Laurent Lamy** (Observatoire de Paris, France),
15 **Adam Masters** (Imperial College London, UK), **Henrik Melin** (University of Leicester, UK), **Julianne Moses**
16 (Space Science Institute, USA), **Oliver Mousis** (Aix Marseille Univ, CNRS, CNES, LAM, Marseille, France),
17 **Nadine Nettleman** (University of Rostock, Germany), **Christina Plainaki** (ASI - Italian Space Agency, Italy),
18 **Jürgen Schmidt** (University of Oulu, Finland), **Amy Simon** (NASA Goddard Space Flight Center, USA), **Gabriel
19 Tobie** (Université de Nantes, France), **Paolo Tortora** (Università di Bologna, Italy), **Federico Tosi** (Istituto
20 Nazionale di AstroFisica – Istituto di Astrofisica e Planetologia Spaziali (INAF-IAPS), Rome, Italy), **Diego Turrini**
21 (Istituto Nazionale di AstroFisica – Istituto di Astrofisica e Planetologia Spaziali (INAF-IAPS), Rome, Italy)

22

23

24 **Abstract:**

25 Uranus and Neptune, and their diverse satellite and ring systems, represent the least explored environments
26 of our Solar System, and yet may provide the archetype for the most common outcome of planetary
27 formation throughout our galaxy. Ice Giants will be the last remaining class of Solar System planet to have a

28 dedicated orbital explorer, and international efforts are under way to realise such an ambitious mission in
29 the coming decades. In 2019, the European Space Agency released a call for scientific themes for its strategic
30 science planning process for the 2030s and 2040s, known as *Voyage 2050*. We used this opportunity to
31 review our present-day knowledge of the Uranus and Neptune systems, producing a revised and updated set
32 of scientific questions and motivations for their exploration. This review article describes how such a mission
33 could explore their origins, ice-rich interiors, dynamic atmospheres, unique magnetospheres, and myriad icy
34 satellites, to address questions at the heart of modern planetary science. These two worlds are superb
35 examples of how planets with shared origins can exhibit remarkably different evolutionary paths: Neptune
36 as the archetype for Ice Giants, whereas Uranus may be atypical. Exploring Uranus' natural satellites and
37 Neptune's captured moon Triton could reveal how Ocean Worlds form and remain active, redefining the
38 extent of the habitable zone in our Solar System. For these reasons and more, we advocate that an Ice Giant
39 System explorer should become a strategic cornerstone mission within ESA's *Voyage 2050* programme, in
40 partnership with international collaborators, and targeting launch opportunities in the early 2030s.

41

42 **Keywords:** Giant Planets; Ice Giants; Robotic Missions; Orbiters; Probes

43

44 1. Introduction: Why Explore Ice Giant Systems?

45 1.1 Motivations

46

47 The early 21st century has provided unprecedented leaps in our exploration of the Gas Giant systems, via the
48 completion of the Galileo and Cassini orbital missions at Jupiter and Saturn; NASA/Juno's ongoing exploration
49 of Jupiter's deep interior, atmosphere, and magnetic field; and ESA's development of the JUICE mission
50 (Jupiter Icy Moons Explorer) to the Galilean satellites. The past decade has also provided our first glimpses
51 of the diversity of planetary environments in the outer solar system, via the New Horizons mission to Pluto.
52 Conversely, the realm of the Ice Giants, from Uranus (20 AU) to Neptune (30 AU), remains largely unexplored,

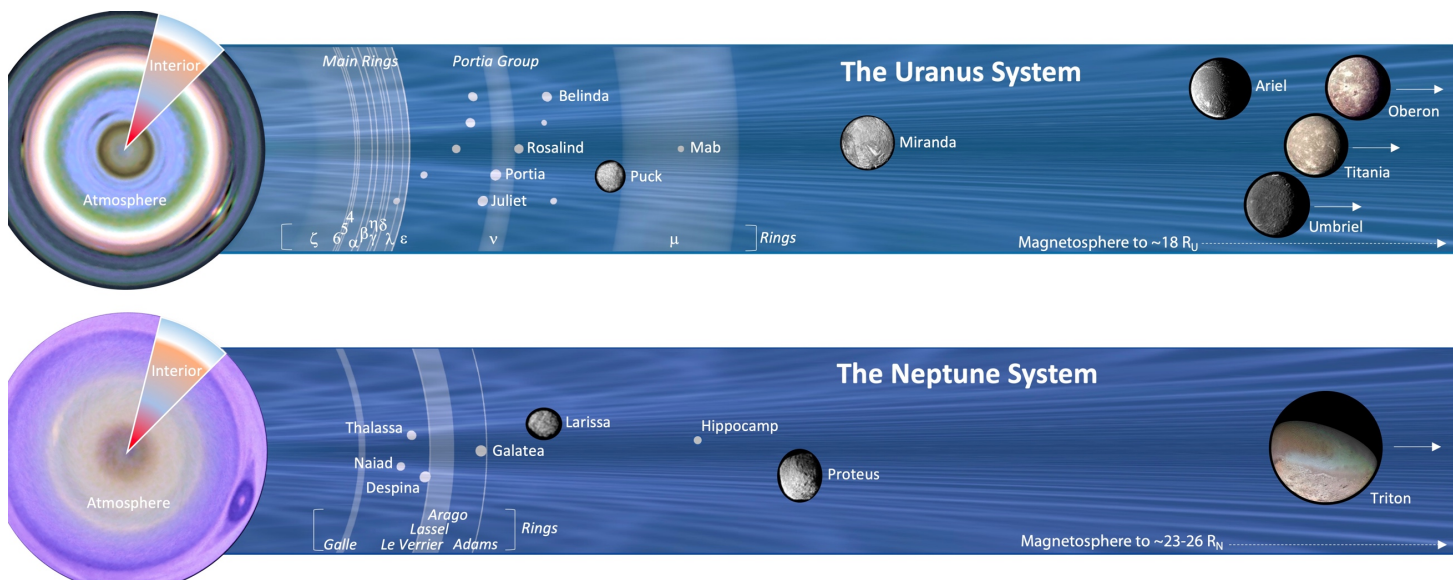


Figure 1 Each Ice Giant exhibits a rich system of planetary environments to explore, from their mysterious interiors, atmospheres and magnetospheres, to the diverse satellites and rings. The inner systems are to scale, with arrows next to major moons indicating that they orbit at larger planetocentric distances. The magnetosphere and radiation belts would encompass the full area of the figure. Credit: L.N. Fletcher/M. Hedman/E. Karkoschka/Voyager-2.

53 each world having been visited only once by a flyby spacecraft – Voyager 2 – in 1986 and 1989 respectively.

54 More than three decades have passed since our first close-up glimpses of these worlds, with cameras,
55 spectrometers and sensors based on 1960s and 70s technologies. Voyager’s systems were not optimised for
56 the Ice Giants, which were considered to be extended mission targets. Uranus and Neptune have therefore
57 never had a dedicated mission, despite the rich and diverse systems displayed in Figure 1. A return to the
58 Ice Giants with an orbiter is the next logical step in humankind’s exploration of our Solar System.

59

60 The Ice Giants may be our closest and best representatives of a whole class of astrophysical objects, as
61 Neptune-sized worlds have emerged as the dominant category in our expanding census of exoplanets (Fulton
62 et al., 2018), intermediate between the smaller terrestrial worlds and the larger hydrogen-rich gas giants
63 (Section 3.3). Our own Ice Giants offer an opportunity to explore physical and chemical processes within
64 these planetary systems as the archetype for these distant exoplanets (Rymer et al., 2018). Furthermore,
65 the formation and evolution of Uranus and Neptune (Section 2.1) pose a critical test of our understanding of
66 planet formation, and of the architecture of our Solar System. Their small size, compared to Jupiter, places
67 strong constraints on the timing of planet formation. Their bulk internal composition (i.e., the fraction of
68 rock, ices, and gases) and the differentiation with depth (i.e., molecular weight gradients, phase transitions

69 to form global water oceans and icy mantles) are poorly known, but help determine the conditions and
70 dynamics in the outer planetary nebula at the time of planet formation.

71

72 Uranus and Neptune also provide two intriguing endmembers for the Ice Giant class. Neptune may be
73 considered the archetype for a seasonal Ice Giant, whereas the cataclysmic collision responsible for Uranus'
74 extreme tilt renders it unique in our Solar System. Contrasting the conditions on these two worlds provides
75 insights into differential evolution from shared origins. The atmospheres of Uranus and Neptune (Section
76 2.2) exemplify the contrasts between these worlds. Uranus' negligible internal heat renders its atmosphere
77 extremely sluggish, with consequences for storms, meteorology, and atmospheric chemistry. Conversely,
78 Neptune's powerful winds and rapidly-evolving storms demonstrates how internal energy can drive powerful
79 weather, despite weak sunlight at 30 AU. Both of these worlds exhibit planetary banding, although the
80 atmospheric circulation responsible for these bands (and their associated winds, temperatures, composition
81 and clouds) remain unclear, and the connection to atmospheric flows below the topmost clouds remains a
82 mystery.

83

84 Conditions within the Ice Giant magnetospheres (Section 2.3) are unlike those found anywhere else, with
85 substantial offsets between their magnetic dipole axes and the planet's rotational axes implying a system
86 with an extremely unusual interaction with the solar wind and internal plasma processes, varying on both
87 rotational cycles as the planet spins, and on orbital cycles.

88

89 The diverse Ice Giant satellites (Section 2.4) and narrow, incomplete ring systems (Section 2.5) provide an
90 intriguing counterpoint to the better-studied Jovian and Saturnian systems. Uranus may feature a natural,
91 primordial satellite system with evidence of extreme and violent events (e.g., Miranda). Neptune hosts a
92 captured Kuiper Belt Object, Triton, which may itself harbour a sub-surface ocean giving rise to active surface
93 geology (e.g., south polar plumes and cryovolcanism).

94

95 Advancing our knowledge of the Ice Giants and their diverse satellite systems requires humankind's first
96 dedicated explorer for this distant realm. Such a spacecraft should combine interior science via gravity and
97 magnetic measurements, *in situ* measurements of their plasma and magnetic field environments, *in situ*
98 sampling of their chemical composition, and close-proximity multi-wavelength remote sensing of the planets,
99 their rings, and moons. This review article will summarise our present understanding of these worlds, and
100 propose a revised set of scientific questions to guide our preparation for such a mission. This article is
101 motivated by ESA's recent call for scientific themes as part of its strategic space mission planning in the period
102 from 2035 to 2050,¹ and is therefore biased to European perspectives on an Ice Giant mission, as explored in
103 the next section.

104

105 1.2 Ice Giants in ESA's Cosmic Vision

106

107 The exploration of the Ice Giants addresses themes at the heart of ESA's existing Cosmic Vision² programme,
108 namely (1) exploring the conditions for planet formation and the emergence of life; (2) understanding how
109 our solar system works; and (3) exploring the fundamental physical laws of the universe. European-led
110 concepts for Ice Giant exploration have been submitted to several ESA Cosmic Vision competitions. The
111 Uranus Pathfinder mission, an orbiting spacecraft based on heritage from Mars Express and Rosetta, was
112 proposed as a medium-class (~€0.5bn) mission in both the M3 (2010) and M4 (2014) competitions (Arridge
113 et al., 2012). However, the long duration of the mission, limited power available, and the programmatic
114 implications of having NASA provide the launch vehicle and radioisotope thermoelectric generators (RTGs),
115 meant that the Pathfinder concept did not proceed to the much-needed Phase A study.

116

117 The importance of Ice Giant science was reinforced by multiple submissions to ESA's call for large-class
118 mission themes in 2013: a Uranus orbiter with atmospheric probe (Arridge et al., 2014), an orbiter to explore

¹ <https://www.cosmos.esa.int/web/voyage-2050>

² <http://sci.esa.int/cosmic-vision/38542-esa-br-247-cosmic-vision-space-science-for-europe-2015-2025/>

119 Neptune and Triton (Masters et al., 2014); and a concept for dual orbiters of both worlds (Turrini et al., 2014).
120 Once again, an ice giant mission failed to proceed to the formal study phase, but ESA's Senior Survey
121 Committee (SSC³) commented that ``*the exploration of the icy giants appears to be a timely milestone, fully*
122 *appropriate for an L class mission. The whole planetology community would be involved in the various aspects*
123 *of this mission... the SSC recommends that every effort is made to pursue this theme through other means,*
124 *such as cooperation on missions led by partner agencies.*''

125

126 This prioritisation led to collaboration between ESA and NASA in the formation of a science definition team
127 (2016-17), which looked more closely at a number of different mission architectures for a future mission to
128 the Ice Giants (Hofstadter et al., 2019). In addition, ESA's own efforts to develop nuclear power sources for
129 space applications have been progressing, with prototypes now developed to utilise the heat from the decay
130 of ²⁴¹Am as their power source (see Section 4.3), provided that the challenge of their low energy density can
131 be overcome. Such an advance might make smaller, European-led missions to the Ice Giants more realistic,
132 and addresses many of the challenges faced by the original Uranus Pathfinder concepts.

133

134 At the start of the 2020s, NASA and ESA are continuing to explore the potential for an international mission
135 to the Ice Giants. A palette of potential contributions (M-class in scale) to a US-led mission have been
136 identified by ESA⁴, and US scientists are currently undertaking detailed design and costing exercises for
137 missions to be assessed in the upcoming US Planetary Decadal Survey (~2022). Each of these emphasise
138 launch opportunities in the early 2030s (Section 4.2), with arrival in the early 2040s (timelines for Ice Giant
139 missions will be described in Section 4.3). This review article summarises those studies, whilst taking the
140 opportunity to update and thoroughly revise the scientific rationale for Ice Giant missions compared to
141 Arridge et al. (2012, 2014), Masters et al. (2014), Turrini et al. (2014) and Hofstadter et al. (2019). We focus
142 on the science achievable from orbit, as the science potential of in situ entry probes has been discussed

³ <http://sci.esa.int/cosmic-vision/53261-report-on-science-themes-for-the-l2-and-l3-missions/>

⁴ <http://sci.esa.int/future-missions-department/61307-cdf-study-report-ice-giants/>

143 elsewhere (Mousis et al., 2018). Section 2 reviews our present-day knowledge of Ice Giant Systems; Section
144 3 places the Ice Giants into their wider exoplanetary context; Section 4 briefly reviews the recent mission
145 concept studies and outstanding technological challenges; and Section 5 summarises our scientific goals at
146 the Ice Giants at the start of the 2020s.

147

148 2. Science Themes for Ice Giant Exploration

149

150 In this section we explore the five multi-disciplinary scientific themes that could be accomplished via
151 orbital exploration of the Ice Giants, and show how in-depth studies of fundamental processes at Uranus and
152 Neptune would have far-reaching implications in our Solar System and beyond. Each sub-section is organised
153 via a series of high-level questions that could form the basis of a mission traceability matrix.

154

155 2.1 Ice Giant Origins and Interiors

156

157 What does the origin, structure, and composition of the two Ice Giants reveal about the formation of
158 planetary systems? Understanding the origins and internal structures of Uranus and Neptune will
159 substantially enhance our understanding of our own Solar System and low-mass exoplanets. Their bulk
160 composition provides crucial constraints on the conditions in the solar nebula during planetary formation
161 and evolution.

162

163 ***How did the Ice Giants first form, and what constraints can be placed on the mechanisms for planetary***
164 ***accretion?*** The formation of Uranus and Neptune has been a long-standing problem for planet formation
165 theory (e.g., Pollack et al., 1996, Dodson-Robinson & Bodenheimer, 2010, Helled & Bodenheimer, 2014). Yet,
166 the large number of detected exoplanets with sizes comparable (or smaller) to that of Uranus and Neptune
167 suggests that such planetary objects are very common (e.g., Batalha et al. 2013), a fact that is in conflict with
168 theoretical calculations.

169

170 The challenge for formation models is to prevent Uranus and Neptune from accreting large amounts of
171 hydrogen-helium (H-He) gas, like the Gas Giants Jupiter and Saturn, to provide the correct final mass and gas-
172 to-solids ratios as inferred by structure models. In the standard planet formation model, core accretion (see
173 Helled et al., 2014 for review and the references therein), a slow planetary growth is expected to occur at
174 large radial distances where the solid surface density is lower, and the accretion rate (of planetesimals) is
175 significantly smaller. For the current locations of Uranus and Neptune, the formation timescale can be
176 comparable to the lifetimes of protoplanetary disks. Due to long accretion times at large radial distances, the
177 formation process is too slow to reach the phase of runaway gas accretion, before the gas disk disappears,
178 leaving behind an intermediate-mass planet (a failed giant planet), which consists mostly of heavy elements
179 and a small fraction of H-He gas.

180

181 However, since the total mass of H-He in both Uranus and Neptune is estimated to be 2-3 Earth masses (M_{\oplus}),
182 it implies that gas accretion had already begun, and this requires that the gas disk disappears at a very specific
183 time, to prevent further gas accretion onto the planets. This is known as the ***fine-tuning*** problem in
184 Uranus/Neptune formation (e.g., Venturini & Helled, 2017). Another possibility is that Uranus and Neptune
185 formed *in situ* within a few Myrs by pebble accretion. In this formation scenario, the core's growth is more
186 efficient than in the planetesimal accretion case, and the pebble isolation mass is above $20 M_{\oplus}$. As a result,
187 the forming planets could be heavy-element dominated with H-He envelopes that are metal-rich due to
188 sublimation of icy pebbles (e.g., Lambrechts et al., 2014).

189

190 Measuring the elemental abundances in the atmospheres of Uranus and Neptune can provide information
 191 on their formation history by setting limits on their formation locations and/or the type of solids
 192 (pebbles/planetesimals) that were accreted. Measurements of the elemental abundances of well-mixed
 193 noble gases, which are only accessible via *in situ* entry probes, would be particularly informative (e.g. Mousis
 194 et al., 2018). In addition, determining the atmospheric metallicity provides valuable constraints for structure
 195 models, as discussed below.

196

197 ***What is the role of giant impacts in explaining the differences between Uranus and Neptune?*** Uranus and
 198 Neptune are somewhat similar in terms of mass and radius, but they also have significant differences such
 199 as their tilt, heat flux, and satellite system. It is possible that these observed differences are a result of giant
 200 impacts that occurred after the formation of the planets (e.g., Safronov 1966, Stevenson 1986). An oblique
 201 impact of a massive impactor can explain Uranus' spin and lead to the formation of a disk where the regular
 202 satellites form. Neptune could have also suffered a head-on impact that could have reached the deep
 203 interior, providing sufficient energy (and mass) to explain the higher heat flux, and possibly the higher mass
 204 and moment of inertia value (e.g., Stevenson 1986, Podolak & Helled, 2012). Giant impact simulations by
 205 various groups confirmed that Uranus' tilt and rotation could be explained by a giant impact (Slattery et al.,

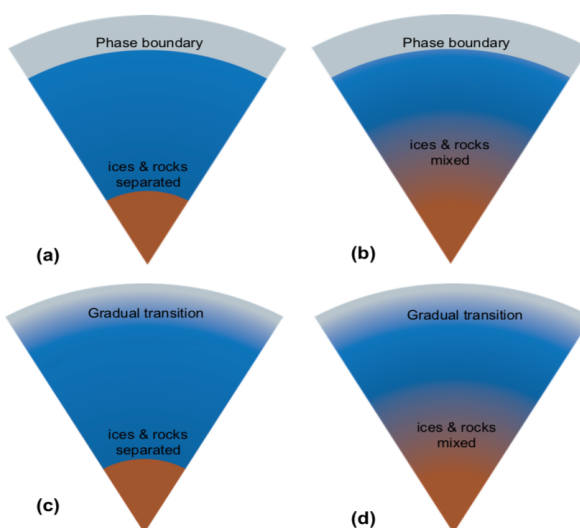


Figure 2 Sketches of the possible internal structures of the ice giants. It is unclear whether the planets are differentiated and whether the transition between the different layers are distinct or gradual: (a) separation between the ices and rocks and the ice and H-He atmosphere (b) separation (phase boundary) between the H-He atmosphere and ices and a gradual transition between ice and rock, (c) gradual transition between the H-He atmosphere and ice layer, and a distinct separation between the ice and rock layers, and (d) gradual transition both between the H-He atmosphere and ice and the ice and rocks suggesting a global composition gradient with the planets (see text for discussion).

206 1992, Kegerreis et al., 2018). Nevertheless, alternative explanations such as orbital migration cannot be
207 excluded (e.g., Boue & Laskar 2010). Understanding the cause of Uranus' tilt and the mechanisms that led to
208 the observed differences between the planets are key questions in planetary science.

209

210 ***What is the bulk composition and internal structure of Uranus and Neptune?*** There are still substantial
211 uncertainties regarding the bulk compositions and internal structures of Uranus and Neptune (e.g., Podolak
212 et al., 1995, Podolak & Helled, 2012, Nettelmann et al., 2013). The available measurements of their physical
213 properties such as mass, radius, rotation rate, atmospheric temperature, and gravitational and magnetic
214 fields are used to constrain models of their interiors. For the Ice Giants, only the gravitational harmonic
215 coefficients J_2 and J_4 are known and their error bars are relatively large (Jacobson, 2009; 2014), nevertheless,
216 various studies have aimed to constrain the planets' internal structures.

217

218 Standard structure models of the planets consist of three layers: a rocky core, an 'icy' shell (water, ammonia,
219 methane, etc.), and a gaseous envelope composed of H-He and heavier elements. The middle layer is not
220 made of "ice" in regard to the physical state of the material (i.e., solid), but is referred to as an icy layer since
221 it is composed of volatile materials such as water, ammonia and methane. The masses and compositions of
222 the layers are modified until the model fits the observed parameters using a physical equation of state (EOS)
223 to represent the materials. Three-layer models predict very high ice-to-rock ratios, where the ice fraction is
224 found to be higher than the rock fraction by 19-35 times for Uranus, and 4-15 times for Neptune, with the
225 total H-He mass typically being 2 and 3 M_{\oplus} for Uranus and Neptune, respectively. The exact estimates are
226 highly model-dependent, and are sensitive to the assumed composition, thermal structure and rotation rate
227 of the planets (Helled et al., 2011, Nettelmann et al., 2013).

228

229 The interiors of Uranus and Neptune could also be more complex with the different elements being mixed,
230 and could also include thermal boundary layers and composition gradients. Indeed, alternative structure
231 models of the planets suggested that Uranus and Neptune could have a density profile without

232 discontinuities (e.g., Helled et al., 2011), and that the planets do not need to contain large fractions of water
233 to fit their observed properties. This alternative model implies that Uranus and Neptune may not be as water-
234 rich as typically thought, but instead are rock-dominated like Pluto (e.g., McKinnon et al., 2017) and could be
235 dominated by composition gradients. It is therefore possible that the “ice giants” are in fact not ice-
236 dominated (see Helled et al., 2011 for details). The very large ice-to-rock ratios found from structure models
237 also suggest a more complex interior structure. At the moment, we have no way to discriminate among the
238 different ice-to-rock ratios inferred from structure models. As a result, further constraints on the gravity and
239 magnetic data (Section 2.3), as well as atmospheric composition and isotopic ratios (e.g., D/H) are required.

240

241 ***How can Ice Giant observations be used to explore the states of matter (e.g., water) and mixtures (e.g.,***
242 ***rocks, water, H-He) under the extreme conditions of planetary interiors?*** In order to predict the mixing
243 within the planets, knowledge from equation-of-state (EOS) calculations is required. Internal structure
244 models must be consistent with the phase diagram of the assumed materials and their mixtures. This is a
245 challenging task and progress in that direction is ongoing. EOS calculations can be used to guide model
246 assumptions. For example, it is possible that Uranus and Neptune have deep water oceans that begin where
247 H₂ and H₂O become insoluble (e.g., Bailey & Stevenson, 2015, Bali et al., 2013). Figure 2 presents sketches
248 of four possible internal structures of the ice giants where the transitions between layers distinct (via
249 phase/thermal boundary) and/or gradual.

250

251 Current observational constraints, foremost J_2 and J_4 , clearly indicate that the deep interior is more enriched
252 in heavy elements than the outer part. Understanding the nature and origin of the compositional gradient
253 zone would yield important information on the formation process and subsequent evolution including
254 possible processes such as outgassing, immiscibility, and sedimentation of ices; processes that play a major
255 role on terrestrial planets and their habitability.

256

257 ***What physical and chemical processes during the planetary formation and evolution shape the magnetic***

258 **field, thermal profile, and other observable quantities?** Structure models must be consistent with the
259 observed multi-polar magnetic fields (see Section 2.3), implying that the outermost ~20% of the planets is
260 convective and consists of conducting materials (e.g., Stanley & Bloxham, 2004, 2006). Currently, the best
261 candidate for the generation of the dynamo is the existence of partially dissociated fluid water in the
262 outermost layers (e.g., Redmer et al., 2011), located above solid and non-convecting superionic water ice
263 ‘mantle’ (Millot et al., 2018). Dynamo models that fit the Voyager magnetic field data suggest the deep
264 interior is stably stratified (Stanley & Bloxham 2004, 2006) or, alternatively, in a state of thermal-buoyancy
265 driven turbulent convection (Soderlund et al., 2013). Improved measurements of the magnetic fields of
266 Uranus and Neptune will also help to constrain the planetary rotation rate. Since Voyager’s measurements
267 of the periodicities in the radio emissions and magnetic fields have not been confirmed by another
268 spacecraft, it is unclear whether the Voyager rotation rate reflects the rotation of the deep interior (Helled
269 et al., 2010), with major consequences for the inferred planetary structure and the question of similar or
270 dissimilar interiors (Nettelmann et al., 2013).

271

272 Finally, the different intrinsic heat fluxes of Uranus and Neptune, together with their similar mass and radius
273 values suggest that the planets formed in a similar way, but then followed different evolutionary histories.
274 Moreover, thermal evolution models that rely on Voyager’s measurements of the albedo, brightness
275 temperatures, and atmospheric pressure-temperature profiles inferred from the occultation data cannot
276 explain both planets with the same set of assumptions.

277

278 Summary: A better understanding of the origin, evolution and structure of Ice Giant planets requires new
279 and precise observational constraints on the planets’ gravity field, rotation rate, magnetic field, atmospheric
280 composition, and atmospheric thermal structure. The insights into origins, structures, dynamo operation
281 and bulk composition provided by an Ice Giant mission would not only shed light on the planet-forming
282 processes at work in our Solar System, but could also help to explain the most common planetary class
283 throughout our observable universe.

284

285 2.2 Ice Giant Atmospheres

286

287 Why do atmospheric processes differ between Uranus, Neptune, and the Gas Giants, and what are the
288 implications for Neptune-mass worlds throughout our Universe? Ice Giant atmospheres occupy a wholly
289 different region of parameter space compared to their Gas Giant cousins. Their dynamics and chemistry are
290 driven by extremes of internal energy (negligible on Uranus, but powerful on Neptune) and extremes of solar
291 insolation (most severe on Uranus due to its 98° axial tilt) that are not seen anywhere else in the Solar System
292 (Figure 3). Their smaller planetary radii, compared to Jupiter and Saturn, affects the width of zonal bands
293 and the drift behaviour of storms and vortices. Their zonal winds are dominated by broad retrograde
294 equatorial jets and do not exhibit the fine-scale banding found on Jupiter, which means that features like
295 bright storms and dark vortices are able to drift with latitude during their lifetimes. Their hydrogen-helium
296 atmospheres are highly enriched in volatiles like CH₄ and H₂S that show strong equator-to-pole gradients,
297 changing the atmospheric density and hence the vertical shear on the winds (Sun et al., 1991). Their
298 temperatures are so low that the energy released from interconversion between different states of hydrogen
299 (ortho and para spin isomers) can play a role in shaping atmospheric dynamics (Smith & Gierasch, 1995).
300 Their middle and upper atmospheres are both much hotter than can be explained by weak solar heating
301 alone, implying a decisive role for additional energy from internal (e.g., waves) or external sources (e.g.,
302 currents induced by complex coupling to the magnetic field). As the **atmospheres are the windows through**
303 **which we interpret the bulk properties of planets**, these defining properties of Ice Giants can provide insights
304 into atmospheric processes on intermediate-sized giant planets beyond our Solar System.

305

306 A combination of global multi-wavelength remote sensing from an orbiter and *in situ* measurements from an
307 entry probe would provide a transformative understanding of these unique atmospheres, focussing on the
308 following key questions (summarised in Figure 3):

309

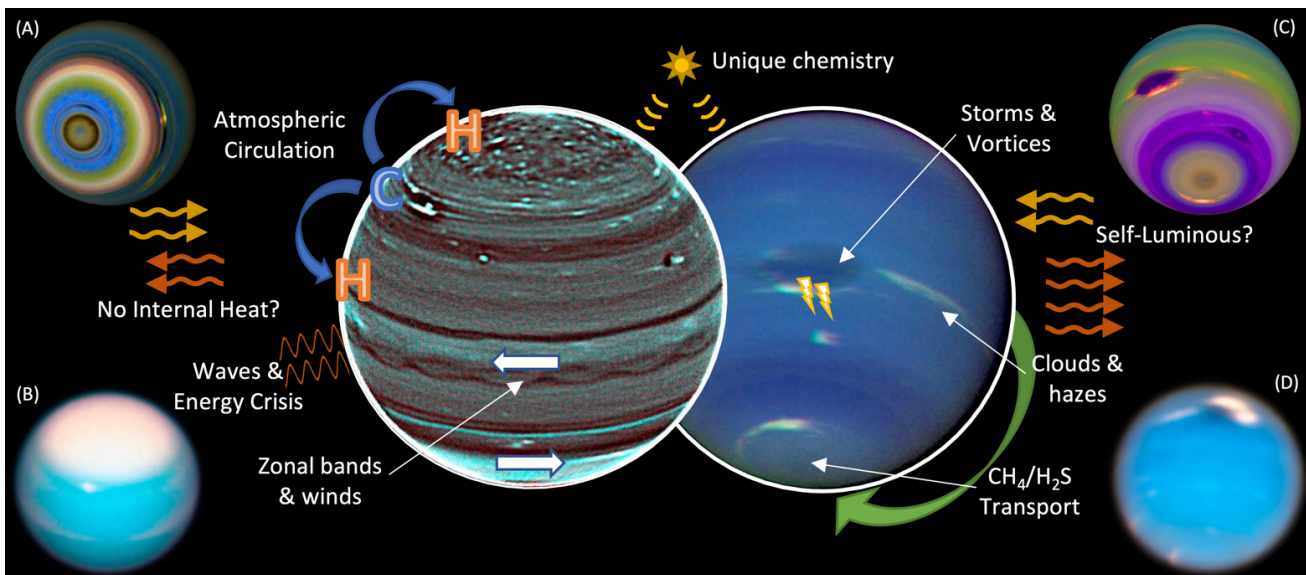


Figure 3 Ice Giant atmospheres are shaped by dynamical, chemical and radiative processes that are not found elsewhere in our Solar System. Images A & C are false-colour representations of Voyager 2 observations of Uranus and Neptune, respectively. Images B and D were acquired by the Hubble Space Telescope in 2018.

310 **What are the dynamical, meteorological, and chemical impacts of the extremes of planetary luminosity?**

311 Despite the substantial differences in self-luminosity (Pearl et al., 1990, 1991), seasonal influences,
 312 atmospheric activity (Sanchez-Lavega et al., 2018), and the strength of vertical mixing (resulting in differences
 313 in atmospheric chemistry, Moses et al., 2018), there are many similarities between these two worlds. In their
 314 upper tropospheres, tracking of discrete cloud features has revealed that both exhibit broad retrograde jets
 315 at their equators and prograde jets nearer the poles, but unlike Jupiter, these are seemingly disconnected
 316 from the fine-scale banding revealed in the visible and near-infrared (Sromovsky et al., 2015). Is this simply
 317 an observational bias, or are winds on the ice giants truly different from those on Jupiter and Saturn? What
 318 sets the scales of the bands? On the Gas Giants, small-scale eddies (from atmospheric instabilities and
 319 convective storms) appear to feed energy into the large-scale winds, but we have never been able to
 320 investigate similar processes on Uranus and Neptune. Indeed, convective processes themselves could be
 321 substantially different – moist convection driven by the condensation of water will likely play a very limited
 322 role in the observable atmosphere, as water is restricted to pressures that exceed tens or hundreds of bars.
 323 Instead, convection may be driven by methane condensation in the 0.1-1.5 bar range (Stoker & Toon, 1989),
 324 or by heat release by ortho-para-H₂ conversion (Smith & Gierasch, 1995). These sources of energy are much
 325 less efficient than those available on Jupiter and Saturn, and the high enrichment in volatiles in the Ice Giants

326 could inhibit vertical motions due to gradients of the atmospheric molecular weight (Guillot et al., 1995;
327 Leconte et al., 2017). Thus, convection may occur in vertically-thin layers (Gierasch et al., 1987), rather than
328 extending vertically over tremendous heights. Multi-wavelength remote sensing of the temperatures,
329 clouds, winds, and gaseous composition is required to investigate how these meteorological processes differ
330 from the Gas Giants, how they derive their energy from the internal heating or weak sunlight, and their
331 relation to the large-scale banded patterns and winds. Spatially-resolved reflectivity and thermal-emission
332 mapping will allow precise constraints on the Ice Giant energy balance to constrain their self-luminosities.
333 And mapping the distribution and depth of Ice Giant lightning, previously detected via radio emissions on
334 both worlds (Zarka et al., 1986; Gurnett et al., 1990), could determine the frequency and intensity of water-
335 powered convection on the Ice Giants, elucidating its impact on their atmospheric dynamics.

336

337 ***What is the large-scale circulation of Ice Giant atmospheres, and how deep does it go?*** Atmospheric
338 circulation, driven by both internal energy and solar heating, controls the thermal structure, radiative energy
339 balance, condensate cloud and photochemical haze characteristics, and meteorology. Unlike Jupiter and
340 Saturn, observations from Voyager, space telescopes, and ground-based observatories have revealed mid-
341 latitude upwelling (where most of the vigorous storms and coolest temperatures are found) and sinking
342 motions at the equator and poles (e.g., Conrath et al., 1998). This is superimposed onto polar depletions in
343 several key cloud-forming volatiles: methane (from reflection spectroscopy, Sromovsky et al., 2014;
344 Karkoschka et al., 2011); hydrogen sulphide (from near-IR and microwave spectroscopy, Hofstadter & Butler,
345 2003, Irwin et al., 2018); and potentially ammonia (from microwave imaging). Do these contrasts imply
346 circulation patterns extending to great depths (de Pater et al., 2014), or are they restricted in vertically-thin
347 layers (Gierasch et al., 1987)? Recent re-analysis of the gravity fields measured by Voyager (Kaspi et al., 2013)
348 suggests that zonal flows are restricted to the outermost ~1000 km of their radii, indicating relatively shallow
349 weather layers overlying the deep and mysterious water-rich interiors. The circulation of the stratosphere is
350 almost entirely unknown on both worlds, due to the challenge of observing weak emissions from
351 hydrocarbons in the mid-infrared (e.g., Orton et al., 2014; Roman et al., 2019). Either way, observations of

352 Uranus and Neptune will have stark implications for atmospheric circulation on intermediate-sized planets
353 with strong chemical enrichments and latitudinal gradients.

354

355 ***How does atmospheric chemistry and haze formation respond to extreme variations in sunlight and vertical***
356 ***mixing, and the influence of external material?*** Methane can be transported into the stratosphere, where
357 photolysis initiates rich chemical pathways to produce a plethora of hydrocarbons (Moses et al., 2018). The
358 sluggish mixing of Uranus indicates that its photochemistry occurs in a different physical regime (higher
359 pressures) than on any other world. Furthermore, oxygen compounds from external sources (from cometary
360 impacts, infalling dust, satellite and ring material, Feuchtgruber et al., 1997) will play different photochemical
361 roles on Uranus, where the methane homopause is lower, than on Neptune (Moses & Poppe, 2017). This
362 exogenic influence can further complicate inferences of planetary formation mechanisms from
363 measurements of bulk abundances (particularly for CO). This rich atmospheric chemistry will be substantially
364 different from that on the Gas Giants, due to the weaker sunlight, the colder temperatures (changing reaction
365 rates and condensation processes), and the unusual ion-neutral chemistry resulting from the complex
366 magnetic field tilt and auroral processes. Condensation of these chemical products (and water ice) can form
367 thin haze layers observed in high-phase imaging (Rages et al., 1991), which may add to the radiative warming
368 of the stratosphere, be modulated by vertically-propagating waves, and could sediment downwards to serve
369 as condensation nuclei or aerosol coatings in the troposphere. Furthermore, Uranus' axial tilt presents an
370 extreme test of coupled chemical and transport models, given that each pole can spend decades in the
371 shroud of winter darkness. The strength of vertical mixing may vary with location, and disequilibrium tracers
372 such as CO (abundant in the tropospheres of Uranus and Neptune, Cavalie et al., 2017), para-H₂ (Conrath et
373 al., 1998) and yet-to-be-detected phosphine (Moreno et al., 2009), arsine, germane, silane, or even
374 tropospheric hydrocarbons (ethane, acetylene), all of which could be used to determine where mixing is most
375 active. Fluorescence spectroscopy, infrared emissions and sub-mm sounding will reveal the vertical,
376 horizontal, and temporal variability of the chemical networks in the unique low-temperature regimes of
377 Uranus and Neptune.

378

379 ***What are the sources of energy responsible for heating the middle- and upper-atmospheres?*** Weak sunlight
380 alone cannot explain the high temperatures of the stratosphere (Li et al., 2018) and thermosphere (Herbert
381 et al., 1987), and this severe deficit is known as the energy crisis. Exploration of Uranus and Neptune may
382 provide a solution to this problem, potentially revealing how waves transport energy vertically from the
383 convective troposphere into the middle atmosphere, and how the currents induced by the asymmetric and
384 time-variable magnetic fields provide energy to the upper atmosphere via Joule heating. For example, the
385 long-term cooling of Uranus' thermosphere, observed via emission from H₃⁺ in the ionosphere (Melin et al.,
386 2019), appears to follow Uranus' magnetic season, which may hint at the importance of particle precipitation
387 modulated by the magnetosphere in resolving the energy crisis. Solving this issue at Uranus or Neptune, via
388 wave observations and exploring magnetosphere-ionosphere-atmosphere coupling processes (e.g., via
389 aurora detected in the UV and infrared), will provide insights into the energetics of all planetary atmospheres.

390

391 ***How do planetary ionospheres enable the energy transfer that couples the atmosphere and***
392 ***magnetosphere?*** In-situ radio occultations remain the only source for the vertical distribution of electron
393 density in the ionosphere (Majeed et al., 2004), a critical parameter for determining the strength of the
394 coupling between the atmosphere and the magnetosphere. The Voyager 2 occultations of both Uranus and
395 Neptune (Lindal et al., 1986, 1992) provided only two profiles for each planet, providing very poor constraints
396 on what drives the complex shape of the electron density profiles in the ionosphere, including the influx of
397 meteoritic material (Moses et al., 2017).

398

399 ***How do Ice Giant atmospheres change with time?*** In the decades since the Voyager encounters, Uranus has
400 displayed seasonal polar caps of reflective aerosols with changing winds (Sromovsky et al., 2015) and long-
401 term upper atmospheric changes (Melin et al., 2019); Neptune's large dark anticyclones – and their
402 associated orographic clouds – have grown, drifted, and dissipated (Lebeau et al., 1998, Stratman et al., 2001,
403 Wong et al., 2018, Simon et al., 2019); and a warm south polar vortex developed and strengthened during

404 the Neptunian summer (Fletcher et al., 2014). What are the drivers for these atmospheric changes, and how
405 do they compare to the other planets? There have been suggestions that storm activity has occurred
406 episodically, potentially with a seasonal connection (de Pater et al., 2015; Sromovsky et al., 2015), but is this
407 simply driven by observational bias to their sunlit hemispheres? Mission scenarios for the early 2040s would
408 result in observations separated from those obtained by the Voyager 2 by 0.5 Uranian years and 0.25
409 Neptunian years. Orbital remote sensing over long time periods, sampling both summer and winter
410 hemispheres, could reveal the causes of atmospheric changes in a regime of extremely weak solar forcing, in
411 contrast to Jupiter and Saturn.

412

413 Summary: Investigations of dynamics, chemistry, cloud formation, atmospheric circulation, and energy
414 transport on Uranus and Neptune would sample a sizeable gap in our understanding of planetary
415 atmospheres, in an underexplored regime of weak seasonal sunlight, low temperatures, and extremes of
416 internal energy and vertical mixing.

417

418 2.3 Ice Giant Magnetospheres

419

420 What can we learn about astrophysical plasma processes by studying the highly-asymmetric, fast-rotating
421 Ice Giant magnetospheres? The off-centered, oblique and fast rotating planetary magnetic fields of Uranus
422 and Neptune give rise to magnetospheres that are governed by large scale asymmetries and rapidly evolving
423 configurations (e.g. Griton et al. 2018), with no other parallels in our Solar System. The solar wind that
424 embeds these two magnetospheres attains Mach numbers significantly larger than those found at Earth,
425 Jupiter, and Saturn, adding further to their uniqueness (Masters et al. 2018). Magnetospheric observations
426 should thus be a high priority in the exploration of the Ice Giants because they extend the sampling of the
427 vast parameter space that controls the structure and evolution of magnetospheres, thus allowing us to
428 achieve a more universal understanding of how these systems work. Insights would also be provided to
429 astrophysical plasma processes on similar systems that are remote to us both in space and time. Such may

430 be the magnetospheres of exoplanets or even that of the Earth at times of geomagnetic field reversals, when
431 the higher order moments of the terrestrial magnetic field become significant, as currently seen at the Ice
432 Giants' (Merrill and Mcfadden, 1999). Evidence for H₃⁺ ionospheric temperature modulations at Uranus due
433 to charged particle precipitation (Melin et al. 2011; 2013) is one of many indications reminding us how strong
434 a coupling between a planet and its magnetosphere can be, and why the study of the latter would be essential
435 also for achieving a system-level understanding of the Ice Giants.

436

437 A synergy between close proximity, remote sensing, and in-situ magnetospheric measurements at the Ice
438 Giants would redefine the state-of-the-art, currently determined by the single Voyager-2 flyby
439 measurements, and limited Earth-based auroral observations. Key questions that would guide such
440 observations are listed below:

441

442 ***Is there an equilibrium state of the Ice Giant magnetospheres?*** Voyager-2 spent only a few planetary
443 rotations within Uranus' and Neptune's magnetopauses, such that it was challenging to establish a nominal
444 configuration of their magnetospheres, their constituent particle populations, supporting current systems
445 and whether these ever approach steady-state. The extent to which the two magnetospheres are modified
446 by internal plasma sources is also poorly constrained; Uranus' magnetosphere for instance was observed to
447 be devoid of any appreciable cold plasma populations (McNutt et al., 1987), although its hydrogen corona is
448 believed to be a major contributor (Herbert et al. 1996). The presence of strong electron radiation belts
449 (Mauk et al. 2010), seems contradictory to the absence of a dense, seed population at plasma energies, or
450 could hint an efficient local acceleration process by intense wave-fields (Scarf et al. 1987). A strong proton
451 radiation belt driven by Galactic Cosmic Ray (GCR)-planet collisions may reside closer to Uranus or Neptune
452 than Voyager-2 reached (e.g. Stone et al. 1986), given that Earth and Saturn, which are known to sustain such
453 belts, are exposed to a considerably lower GCR influx than the Ice Giants (Buchvarova and Belinov, 2009). Ion
454 composition and UV aurora measurements hint that Triton could be a major source of plasma in Neptune's
455 magnetosphere (Broadfoot et al., 1989, Richardson & McNutt, 1990), although questions remain as to the

456 effects of coupling between the magnetosphere and the moon's atmosphere and ionosphere in establishing
457 the plasma source (Hoogeveen & Cloutier, 1996). The magnetotails of both planets are expected to have very
458 different structures to those seen at other magnetized planets (Figure 4), with strong helical magnetic field
459 components (Cowley, 2013; Griton and Pantellini 2020), that may lead to a similarly helical topology of
460 reconnection sites across the magnetospheric current sheet (Griton et al. 2018). Whether the overall
461 magnetospheric configuration is controlled more by current sheet reconnection or a viscous interaction
462 along the magnetopause (Masters et al. 2018) is also unknown. Finally, measuring average escape rates of
463 ionospheric plasma would offer further insights on whether planetary magnetic fields protect planetary
464 atmospheres from solar wind erosion (Wei et al. 2014, Gunell et al., 2018). For such dynamic systems, long-
465 term observations that average out rotational effects and transients (e.g. Selesnick, 1988) are essential for
466 achieving closure to all the aforementioned questions.

467

468 ***How do the Ice Giant magnetospheres evolve dynamically?*** The large tilts of the Ice Giant magnetic fields
469 relative to their planetary spin-axes hint that large-scale reconfigurations at diurnal time scales are
470 dominating short-term dynamics, a view supported by MHD simulations (Griton and Pantellini 2020; Griton
471 et al. 2018; Cao and Paty 2017; Mejnertsen et al. 2016). The rate of magnetic reconnection, for instance, is
472 predicted to vary strongly with rotation, and so is the rate of matter and energy transfer into the
473 magnetosphere and eventually upper atmosphere (Masters et al., 2014). Simulations do not capture how
474 such variations impact regions as the radiation belts, which would typically require a stable environment to
475 accumulate the observed, high fluxes of energetic particles (Mauk et al. 2010). A strong diurnal variability
476 may also affect the space weather conditions at the orbits of the Ice Giant moons, regulating the interactions
477 between the charged particle populations, their surfaces and exospheres (Plainaki et al., 2016; Arridge et al.,
478 2014) through processes like surface sputtering, ion pick up, and charge exchange, which may also feed the
479 magnetosphere with neutrals and low energy, heavy ion plasma (Lammer 1995). In the time-frame
480 considered here, the exploration of Neptune could provide an opportunity to study a “pole-on”
481 magnetosphere at certain rotational phases.

482

483 Additional sources of variability can be solar wind driven, such as Corotating Interaction Regions (CIRs) and
484 Interplanetary Coronal Mass Ejections (ICMEs) (Lamy et al. 2017). By the time they reach Uranus and
485 Neptune, ICMEs expand and coalesce and attain a quasi-steady radial width of ~2-3 AU (Wang and
486 Richardson, 2004) that could result in active magnetospheric episodes with week-long durations. With Triton
487 being a potential active source, Neptune's magnetosphere may show variations at the moon's orbital period
488 (Decker and Cheng 1987).

489

490 On longer time scales, seasonal changes of the planetary field's orientation are most important, especially at
491 Uranus, because of its spin axis which almost lies on the ecliptic. There may be additional implications for the
492 long-term variability of the magnetosphere if magnetic field measurements reveal a secular drift of the
493 planetary field at any of the Ice Giants, in addition to providing constraints on the magnetic fields' origin and
494 the planets' interiors (Section 2.1).

495

496 ***How can we probe the Ice Giant magnetospheres through their aurorae?*** Aurorae form a unique diagnostic
497 of magnetospheric processes by probing the spatial distribution of active magnetospheric regions and their
498 dynamics at various timescales. Auroral emissions of Uranus and Neptune were detected by Voyager 2 at
499 ultraviolet and radio wavelengths. The Uranian UV aurora has been occasionally re-detected by the Hubble
500 Space Telescope since then. At NIR wavelengths auroral signatures remain elusive (e.g. Melin et al., 2019).

501

502 UV aurora are collisionally-excited H Ly- α and H₂ band emissions from the upper atmosphere, driven by
503 precipitating energetic particles. The radical differences of the Uranian UV aurora observed across different
504 seasons were assigned to seasonal variations of the magnetosphere/solar wind interaction (Broadfoot et al.,
505 1986; Lamy et al., 2012, 2017; Cowley, 2013; Barthélémy et al., 2014). The tentative detection of Neptunian
506 UV aurora did not reveal any clear planet-satellite interaction (e.g. with Triton) (Broadfoot et al., 1989).

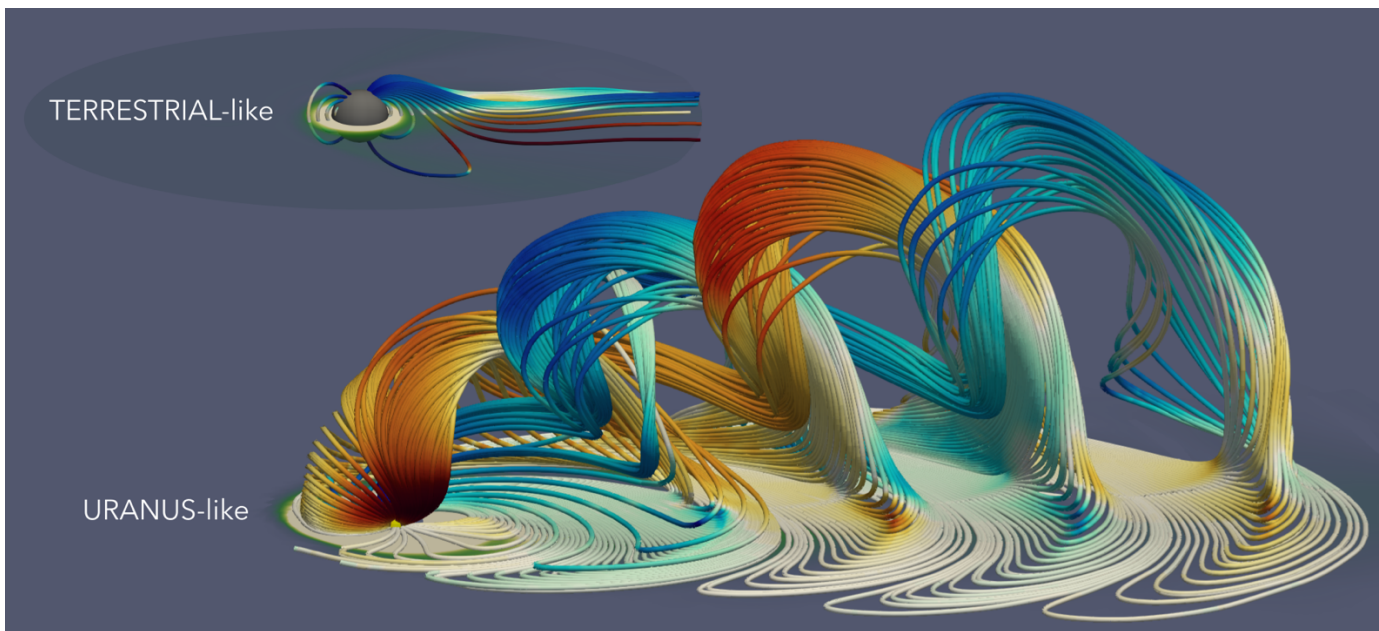


Figure 4 Typical magnetic field configuration in a terrestrial-like, solar wind driven magnetosphere (top) where the magnetic and spin axis are almost aligned, compared to a Uranus-like magnetospheric configuration (bottom), when the magnetic axis is 90° away from the spin axis, during equinox. The helicoidal magnetotail structure develops due to the planet's fast rotation.

507 Repeated UV spectro-imaging observations are essential to probe the diversity of Ice Giant aurora, assess
 508 their underlying driver and constrain magnetic field models (e.g. Herbert, 2009).

509

510 Uranus and Neptune produce powerful auroral radio emissions above the ionosphere most likely driven by
 511 the Cyclotron Maser Instability as at Earth, Jupiter, and Saturn. The Uranian and Neptunian Kilometric
 512 Radiation are very similar (Desch et al., 1991, Zarka et al., 1995). They include (i) bursty emissions (lasting for
 513 <10min) reminiscent of those from other planetary magnetospheres. A yet-to-be-identified time-stationary
 514 source of free energy, able to operate in strongly variable magnetospheres, is thought to drive (ii) smoother
 515 emissions (lasting for hours) that are unique in our solar system (Farrell, 1992). Long-term remote and in-situ
 516 radio measurements are crucial to understand the generation of all types of Ice Giant radio emissions, to
 517 complete the baseline for the search of exoplanetary radio emissions. Long-term monitoring of auroral
 518 emissions will also be essential to precisely determine the rotation periods of these worlds.

519

520 Summary: The Ice Giant magnetospheres comprise unique plasma physics laboratories, the study of which
 521 would allow us to observe and put to test a variety of astrophysical plasma processes that cannot be resolved
 522 under the conditions that prevail at the terrestrial planets and at the Gas Giants. The strong planet-

523 magnetosphere links that exist further attest to the exploration of the magnetospheres as a key ingredient
524 of the Ice Giant systems.

525

526 [2.4 Ice Giant Satellites – Natural & Captured](#)

527

528 What can a comparison of Uranus' natural satellites and the captured "Ocean World" Triton reveal about the
529 drivers of active geology and potential habitability throughout the outer Solar System? The satellite systems
530 of Uranus and Neptune offer very different insights into moon formation and evolution; they are microcosms
531 of the larger formation and evolution of planetary systems. The Neptunian system is dominated by the
532 cuckoo-like arrival of Triton, which would be the largest known dwarf planet in the Kuiper belt if it were still
533 only orbiting the Sun. Neptune's remaining satellites may not be primordial, given the degree of system
534 disruption generated by Triton's arrival. In contrast, Uranus's satellite system appears to be relatively
535 undisturbed since its formation — a highly surprising situation given that Uranus has the most severe axial
536 tilt of any planet, implying a dramatic collisional event in its past. Thus, these two satellite systems offer
537 laboratories for understanding the key planetary processes of formation, capture and collision.

538

539 ***What can the geological diversity of the large icy satellites of Uranus reveal about the formation and***
540 ***continued evolution of primordial satellite systems?*** The five largest moons of Uranus (Miranda, Ariel,
541 Umbriel, Titania, Oberon) are comparable in sizes and orbital configurations to the medium-sized moons of
542 Saturn. However, they have higher mean densities, about 1.5 g/cm^3 on average, and have different insolation
543 patterns: their poles are directed towards the Sun for decades at a time, due to the large axial tilt of Uranus.
544 The surfaces of Uranus's five mid-sized moons exhibit extreme geologic diversity, demonstrating a complex
545 and varied history (Figure 1). On Ariel and Miranda, signs of endogenic resurfacing associated with tectonic
546 stress, and possible cryovolcanic processes, are apparent: these moons appear to have the youngest
547 surfaces. Geological interpretation has suffered greatly from the incomplete Voyager 2 image coverage of
548 only the southern hemisphere, and extremely limited coverage by Uranus-shine in part of the north (Stryk

549 and Stooke, 2008). Apart from a very limited set of images with good resolution at Miranda, revealing
550 fascinatingly complex tectonic history and possible re-formation of the moon (Figure 5), most images were
551 acquired at low to medium resolution, only allowing characterisation of the main geological units (e.g., Croft
552 and Soderblom, 1991) and strongly limiting any surface dating from the crater-size frequency distribution
553 (e.g. Plescia, 1987a, Plescia, 1987b). High-resolution images of these moons, combined with spectral data,
554 will reveal essential information on the tectonic and cryovolcanic processes and the relative ages of the
555 different geological units, via crater statistics and sputtering processes. Comparison with Saturn's inner
556 moons system will allow us to identify key drivers in the formation and evolution of compact multiplanetary
557 systems.

558

559 ***What was the influence of tidal interaction and internal melting on shaping the Uranian worlds, and could
560 internal water oceans still exist?*** As in the Jovian and Saturnian systems, tidal interaction is likely to have
561 played a key role in the evolution of the Uranian satellite system. Intense tidal heating during sporadic
562 passages through resonances is expected to have induced internal melting in some of the icy moons
563 (Tittemore and Wisdom 1990). Such tidally-induced melting events, comparable to those expected on
564 Enceladus (e.g. Běhounková et al. 2012), may have triggered the geological activity that led to the late
565 resurfacing of Ariel and possibly transient hydrothermal activity. The two largest (>1500 km diameter)
566 moons, Titania and Oberon, may still harbour liquid water oceans between their outer ice shells and inner
567 rocky cores – remnants of past melting events. Comparative study of the static and time-variable gravity field
568 of the Uranian and Saturnian moons, once well-characterized, will constrain the likelihood and duration of
569 internal melting events, essential to characterize their astrobiological potential. Complete spacecraft
570 mapping of their surfaces could reveal recent endogenic activity.

571

572 Accurate radio tracking and astrometric measurements can also be used to quantify the influence of tidal
573 interactions in the system at present, providing fundamental constraints on the dissipation factor of Uranus
574 itself (Lainey, 2008). Gravity and magnetic measurements, combined with global shape data, will greatly

575 improve the models of the satellites' interiors, providing fundamental constraints on their bulk composition
576 (density) and evolution (mean moment of inertia). Understanding their ice-to-rock ratio and internal
577 structure will enable us to understand if Uranus' natural satellite system are the original population of bodies
578 that formed around the planet, or if they were disrupted.

579

580 ***What is the chemical composition of the surfaces of the Uranian moons?*** The albedos of the major Uranian
581 moons, considerably lower than those of Saturn's moons (except Phoebe and Iapetus's dark hemisphere),
582 reveal that their surfaces are characterized by a mixture of H₂O ice and a visually dark and spectrally bland
583 material that is possibly carbonaceous in origin (Brown and Cruikshank, 1983). Pure CO₂ ice is concentrated
584 on the trailing hemispheres of Ariel, Umbriel and Titania (Grundy et al., 2006), and it decreases in abundance
585 with increasing semimajor axis (Grundy et al., 2006; Cartwright et al., 2015), as opposed to what is observed
586 in the Saturnian system. At Uranus' distance from the Sun, CO₂ ice should be removed on timescales shorter
587 than the age of the Solar System, so the detected CO₂ ice may be actively produced (Cartwright et al., 2015).

588

589 The pattern of spectrally red material on the major moons will reveal their interaction with dust from the
590 decaying orbits of the irregular satellites. Spectrally red material has been detected primarily on the leading
591 hemispheres of Titania and Oberon. H₂O ice bands are stronger on the leading hemispheres of the classical
592 satellites, and the leading/trailing asymmetry in H₂O ice band strengths decreases with distance from Uranus.
593 Spectral mapping of the distribution of red material and trends in H₂O ice band strengths across the satellites
594 and rings can map out infalling dust from Uranus's inward-migrating irregular satellites (Cartwright et al.,
595 2018), similar to what is observed in the Saturnian system on Phoebe/Iapetus (e.g., Tosi et al., 2010), and
596 could reveal how coupling with the Uranus plasma and dust environment influence their surface evolution.

597

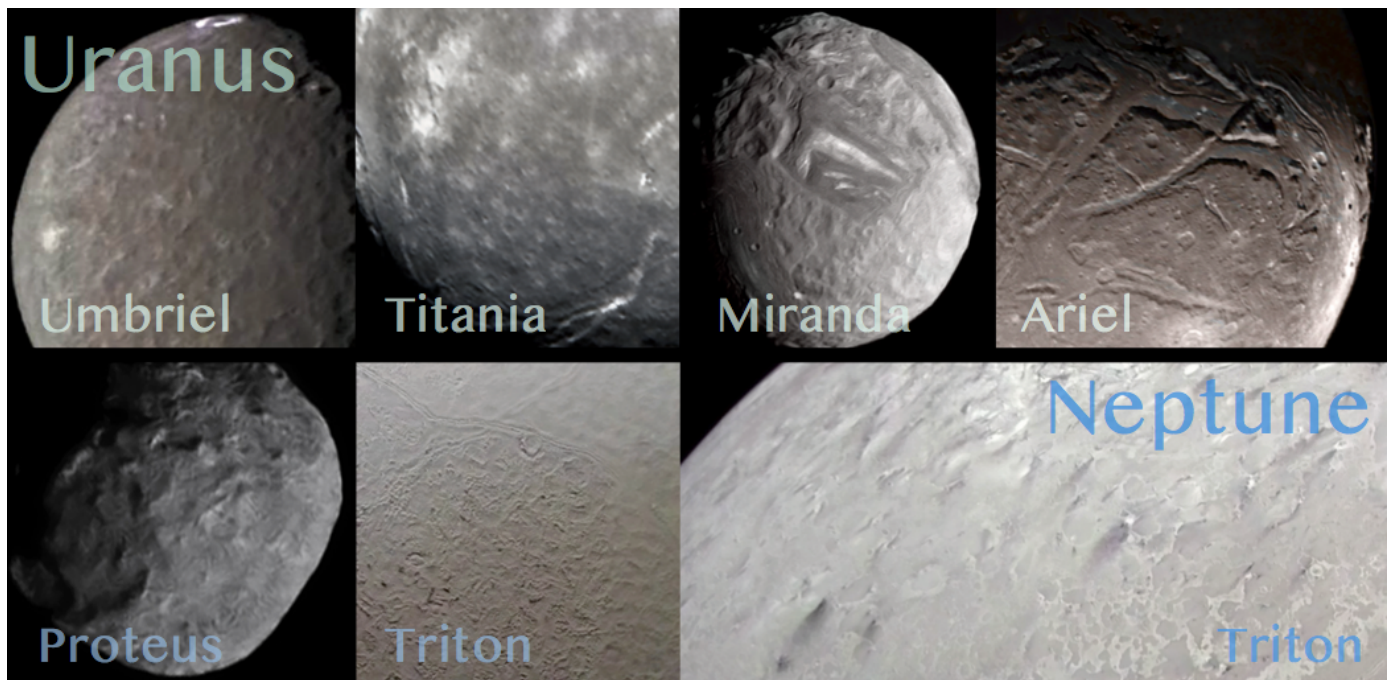


Figure 5 Best-resolution (roughly ~1 km/px) imagery of terrains seen in the moons of Uranus (top row) and Neptune (lower row) by Voyager 2. At Uranus, Umbriel and Titania are highly cratered with some major faults; Miranda displays spectacular and massive tectonic features; Ariel's filled-fissured surface is suggestive of late cryovolcanic activity. At Neptune, Proteus has a surface suggestive of Saturn's dust-rich moon Helene. The dwarf-planet-sized Triton has both the sublimation-related "cantaloupe terrain" (left) and active nitrogen gas geysers in the south polar terrains (right), with deposited dust visible as dark streaks. Credit: NASA/JPL-Caltech/Ted Stryk/collage M. Bannister.

598 **Does Triton currently harbour a subsurface ocean and is there evidence for recent, or ongoing, active**

599 **exchange with its surface?** The large moon Triton, one of a rare class of Solar System bodies with a

600 substantial atmosphere and active geology, offers a unique opportunity to study a body comparable to the

601 dwarf planets of the rest of the trans-Neptunian region, but much closer. Triton shares many similarities in

602 surface and atmosphere with Pluto (Grundy et al. 2016), and both may harbour current oceans. Triton's

603 retrograde orbit indicates it was captured, causing substantial early heating. Triton, in comparison with

604 Enceladus and Europa, will let us understand the role of tidally-induced activity on the habitability of ice-

605 covered oceans. The major discovery of plumes emanating from the southern polar cap of Triton (Soderblom

606 et al. 1990; see Figure 5) by Voyager 2, the most distant activity in the Solar System, is yet to be fully

607 understood (Smith et al. 1989).

608

609 Like Europa, Triton has a relatively young surface age of ~100 Ma (Stern and McKinnon 2000), inferred from

610 its few visible impact craters. Triton also displays a variety of distinctive curvilinear ridges and associated

611 troughs, comparable to those on Europa (Prockter et al. 2005) and especially apparent in the "cantaloupe

612 terrain". This suggests that tidal stresses and dissipation have played an essential role in Triton's geological
613 activity, and may be ongoing (Nimmo and Spencer 2015). Intense tidal heating following its capture could
614 have easily melted its icy interior (McKinnon et al. 1995). Its young surface suggests that Triton experienced
615 an ocean crystallization stage relatively recently (Hussmann et al. 2006), associated with enhanced surface
616 heat flux (Martin-Herrero et al. 2018). Combined magnetic, gravimetric and shape measurements from
617 multiple flybys or in orbit will allow us to detect if Triton possesses an ocean and to constrain the present-
618 day thickness of the ice shell. Correlating the derived shell structure and geological units will show if there is
619 exchange with the ocean. It is entirely unclear if the source(s) for Triton's plumes reaches the ocean, as at
620 Enceladus.

621

622 ***Are seasonal changes in Triton's tenuous atmosphere linked to specific sources and sinks on the surface,***
623 ***including its remarkable plume activity?*** Triton's surface has a range of volatile ices seen in Earth-based
624 near-infrared spectra, including N₂, H₂O, CO₂, and CH₄ (Quirico et al., 1999; Cruikshank et al., 2000; Tegler et
625 al, 2012). A 2.239 μm absorption feature suggests that CO and N₂ molecules are intimately mixed in the ice
626 rather than existing as separate regions of pure CO and pure N₂ deposits (Tegler et al., 2019). Mapping the
627 spatial variation of this absorption feature will constrain how the surface-atmosphere interaction affects the
628 surface composition, and more generally its climate and geologic evolution. Triton's surface may also contain
629 complex organics from atmospheric photochemistry, like those of Pluto or Saturn's moon Titan (e.g.
630 Krasnopolsky and Cruikshank 1995), as suggested by its yellowish areas (Thompson and Sagan 1990).
631 Identifying the organic compounds, and mapping out their correlation with recently active terrains and
632 geysers, will strongly raise the astrobiological potential of this exotic icy world.

633

634 Triton's tenuous atmosphere is mainly molecular nitrogen, with a trace of methane and CO near the surface
635 (Broadfoot et al. 1989, Lellouch et al. 2010). Despite Triton's distance from the Sun and its cold temperatures,
636 the weak sunlight is enough to drive strong seasonal changes on its surface and atmosphere. Because CO and
637 N₂ are the most volatile species on Triton, they are expected to dominate seasonal volatile transport across

638 its surface. Observation of increased CH₄ partial pressure between 1989 and 2010 (Lellouch et al. 2010)
639 confirmed that Triton's atmosphere is seasonably variable. The plumes of nitrogen gas and dust could be a
640 seasonal solar-driven process like the CO₂ 'spiders' of the south polar regions of Mars, although an endogenic
641 origin is possible.

642

643 ***Are the smaller satellites of Neptune primordial?*** Voyager 2's flyby led to the discovery of six small moons
644 inside Triton's orbit: Naiad, Thalassa, Despina, Galatea, Larissa and Proteus. A seventh inner moon,
645 Hippocamp, has been recently discovered by HST observations orbiting between the two largest, Larissa and
646 Proteus. Almost nothing is known about these faint moons, which may post-date Triton's capture rather than
647 being primordial. Only a new space mission could unveil basic features such as shape and surface
648 composition, shedding light on their origin.

649

650 ***How does an Ice Giant satellite system interact with the planets' magnetospheres?*** Most of the major
651 moons of Uranus and Neptune orbit within the planets' extensive magnetospheres (Figure 1). The tilt and
652 offset of both planets' magnetic dipoles compared to their rotation axes mean that, unlike at Saturn, the
653 major moons at both Ice Giants experience continually-changing external magnetic fields. The potential
654 subsurface oceans of Titania, Oberon and Triton would be detectable by a spacecraft that can monitor for an
655 induced magnetic field. The moons in both systems orbit in relatively benign radiation environments, but
656 radiation belt particles could still drive sputtering processes at the inner moons' surfaces and Triton's
657 atmosphere. Triton could be a significant potential source of a neutral gas torus and magnetospheric plasma
658 at Neptune. Triton's ionosphere's transonic, sub-Alfvenic regime (Neubauer 1990; Strobel et al. 1990) may
659 generate an auroral spot in Neptune's upper atmosphere. No such interaction is anticipated at Uranus. Red
660 aurorae may also be present on Triton from N₂ emission, providing valuable insights into Triton's interaction
661 with its space environment.

662

663 Summary: Exploring Uranus' natural satellites and Neptune's captured moon Triton will reveal how ocean
664 worlds may form and remain active, defining the extent of the habitable zone in the Solar System.

665

666 [2.5 Ice Giant Ring Systems](#)

667

668 What processes shape the narrow, dusty rings of Ice Giants, and why do they differ from the extensive rings
669 of Saturn? Uranus and Neptune both possess a complex system of rings and satellites (Figure 6). The rings
670 exhibit narrow and dense ringlets, as well as fainter but broader dust components. The moons can confine
671 the rings gravitationally, and may also serve as sources and sinks for ring material. Observations indicate
672 rapid variability in the Uranian and Neptunian rings within decades. A mission to the Ice Giants, with a
673 dedicated suite of instruments, can answer fundamental questions on the formation and evolution of the
674 ring systems and the planets themselves:

675

676 ***What is the origin of the solar system ring systems, and why are they so different?*** The origin of the giant
677 planets' rings is one of the unsolved mysteries in planetary science. Whereas all four giant planets do have
678 rings, their diversity of structure and composition argues for different formation scenarios. It was
679 hypothesized that the very massive Saturnian rings formed more than 3 Gyrs ago through tidal destruction
680 of a moon, or of a body on a path traversing the system. However, recent Cassini measurements (Zhang et
681 al., 2017, Kempf et al., 2018, Waite et al., 2018, Iess et al., 2019) argue for a younger ring age. In contrast,
682 Uranus' and Neptune's rings are far less massive and they have a different structure. Compared to Saturn,
683 their rings' albedo is much lower, favouring a parent body that was a mixture of ice and dark material
684 (silicates and possibly organics). For instance, it was suggested (Colwell and Esposito, 1992, 1993) that these
685 two ring systems could result from the periodic destruction of moonlets though meteoroid bombardment,
686 in which case most of the ringlets would be only transient because of re-accretion processes. Among the
687 Uranian dust rings the μ ring has a distinct blue spectral slope (de Pater et al. 2006). In that regard it is similar
688 to Saturn's E ring, for which the blue slope results from the narrow size distribution of its grains, formed in

689 the cryo-volcanic activity of the moon Enceladus. Although the moon Mab is embedded in the μ ring
690 (Showalter et al, 2006) it appears much too small (12km radius) to be volcanically active and create in this
691 way the dust that forms the ring. Other dust rings of Uranus exhibit a red spectral slope (de Pater et al. 2006),
692 suggestive of dusty material released in micrometeoroid impacts on atmosphere-less moons and the origin
693 for different appearance of the μ ring is unknown. Recent ground-based observations of thermal emission
694 from the Uranian ring system (Molter et al., 2019) are consistent with the idea that the rings are made up of
695 larger particles, without micron-sized dust, and that their temperatures result from low thermal inertia
696 and/or slow rotation of the particles. Clearly, more data is needed to ultimately settle the question of the
697 origin and nature of Uranus' and Neptune's rings.

698

699 **How do the ring-moon systems evolve?** A variety of processes govern the evolution of planetary rings, many
700 of which are also fundamental to other cosmic disks. Important for the rings are viscous transport, ring-
701 satellite interactions, the self-gravity, as well as meteoroid bombardment and cometary impacts. These
702 processes may induce rapid evolution on timescales much shorter than the rings' age. For instance, the
703 Neptune ring arcs were initially interpreted to be confined by resonances with the moon Galatea. However,
704 it was found that the arcs actually move away from the corresponding corotation sites (Dumas et al., 1999,
705 Namouni & Porco 2002) and that they evolve rapidly (de Pater et al., 2005). Also, for the Uranian rings
706 significant changes since the Voyager epoch are observed (de Pater et al., 2006, 2007). In the Uranus and
707 Neptune systems the role the moons play in sculpting the rings is even stronger than for Saturn's rings.
708 Moreover, depending on their composition, the Uranus and Neptune ring systems may even extend beyond
709 the planet's Roche Limit (Tiscareno et al., 2013). This implies that their path of evolution is different from the
710 Saturnian rings, inducing changes on more rapid timescales. Some of the edges of the Uranian rings are
711 clearly confined by known satellites and others might be confined by yet undetected moons. Alternatively,
712 there might be different processes of confinement at work, in a similar manner as for narrow rings of Saturn,
713 for which shepherding moons are absent. Some of the dense rings of Uranus show sub-structure the origin

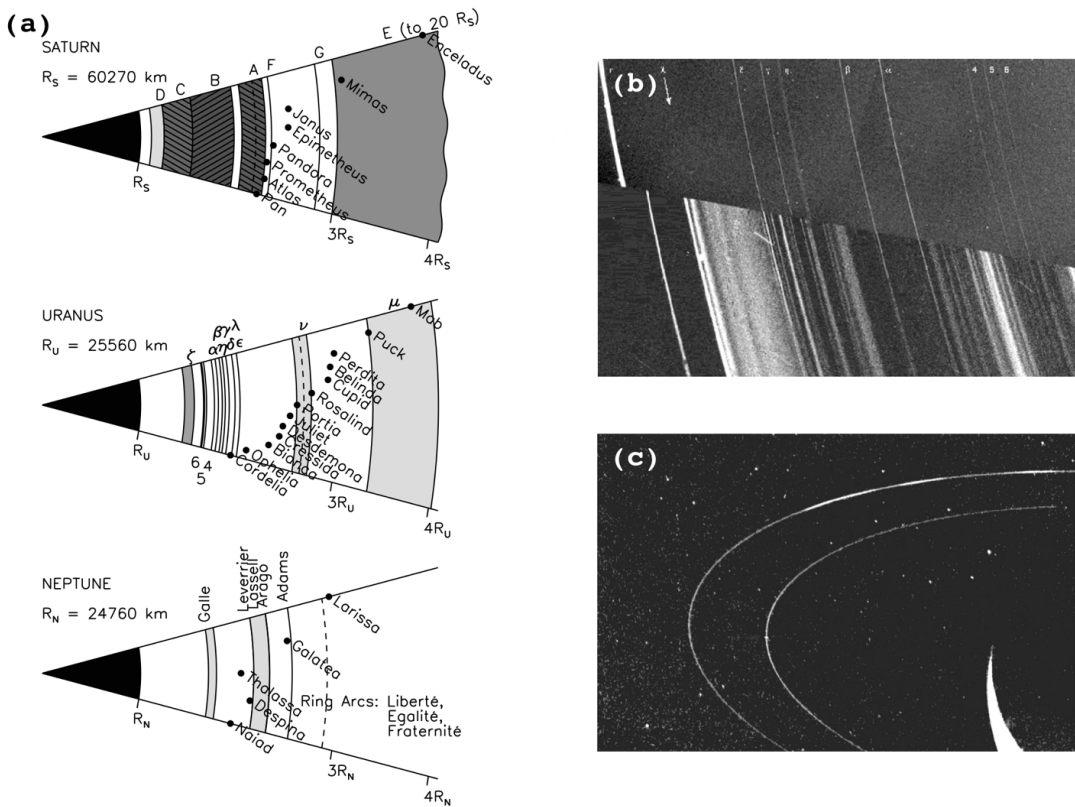


Figure 6 Panel (a): Schematic diagram of the ring moon systems of Uranus, Neptune, and Saturn for comparison. The Roche radius (for icy ring particles) is marked as a dashed line. Panel (b) shows a combination of two Voyager images of the Uranus rings, taken at low (upper part) and high (lower part) phase angle. At high phase angle the dusty components of the ring system stand out (IMAGES: NASA/JPL). Panel (c) shows a Voyager image of the rings of Neptune (IMAGES: NASA/JPL).

714 of which is unclear. Spacecraft investigation will answer the question if the structure is induced by resonant
 715 interaction with moons, or if it represents intrinsic modes arising from instability and self-gravity of the rings.

716

717 **What is the ring composition?** The rings (as the moons) very likely consist of material that was present at
 718 the location in the solar system where the planets themselves have formed. Therefore, the investigation of
 719 the composition of the rings, while being interesting in its own right, may also shed light on models of planet
 720 formation and migration in the solar system. Imaging at high and intermediate phase angles will constrain
 721 the shapes and properties of known dust rings and has the potential to discover new rings. Multicolour
 722 imaging at a range of phase angles will determine the size distribution of the grains that form these rings.
 723 Imaging at low phase angles will probe the dense rings and allow for a comprehensive search and discovery
 724 of yet unseen satellites that serve as sources for ring material and that interact dynamically with the rings.
 725 Stellar occultations performed with a high-speed photometer, or radio occultations, will determine the
 726 precise optical depths of the denser rings and resolve their fine sub-structure (French et al., 1991). An IR

727 spectrometer will determine the composition of the dense rings. In a complementary manner a dust detector
728 will directly determine the composition of the grains forming the low optical depth dust rings (Postberg et
729 al., 2009) and of particles lifted from the dense rings (Hsu et al., 2018).

730

731 Summary: Ice Giant rings appear to be fundamentally different to those of Saturn, such that their origin,
732 evolution, composition and gravitational relationships with the icy satellites should provide key new insights
733 into the forces shaping ring systems surrounding planetary bodies.

734 3. Ice Giant Science in Context

735

736 The scientific themes highlighted in Section 2 span multiple disciplines within planetary science, and address
737 questions that touch on issues across astronomy. In this section we review how an Ice Giant mission must
738 be considered in the context of other fields and technologies that will be developing in the coming decades.

739

740 3.1 Astronomical Observatories

741

742 An Ice Giant System mission would be operating in the context of world-leading new facilities on or near
743 Earth. The 2020s will see the launch of the James Webb Space Telescope, able to provide spectral maps of
744 both Ice Giants from 1-30 μm but at a moderate spatial resolution and with limited temporal coverage. Earth-
745 based observatories in the 8-10 m class provide better spatial resolution at the expense of telluric
746 obscuration. A successor to the Hubble Space Telescope, which has been the key provider of visible and UV
747 observations of the Ice Giants, has yet to become a reality, but could be operating in the 2030s. And although
748 the next generation of Earth-based observatories in the 30+m class (the ELT, TMT, GMT) will provide exquisite
749 spatial resolution, this will remain limited to atmospheric and ionospheric investigations of the Earth-facing
750 hemisphere (with some disc-averaged spectroscopy of the satellites), leaving a multitude of fundamental
751 questions unanswered.

752

753 Additionally, distant remote sensing can only study phenomena that alter the emergent spectrum –
754 meteorology, seasonal variations, and ionospheric emissions (auroral and non-auroral). This limits our
755 understanding of the underlying mechanisms and means that ground- and space-based telescopes only serve
756 a narrow subset of the Ice Giant community, and cannot address the wide-ranging goals described in Section
757 2. Thus, there is no substitute for orbital exploration of one or both of these worlds, but we envisage that
758 these space missions will work in synergy with the ground-based astronomy community, following successful
759 examples of Galileo, Cassini, Juno and, ultimately, JUICE and Europa Clipper. Support from Earth-based
760 observatories, either on the ground or in space, will be used to establish a temporal baseline for atmospheric
761 changes (e.g., tracking storms), provide global context for close-in observations from the orbiters, and plug
762 any gaps in spectral coverage or spectral resolution in the orbiter payload.

763

764 3.2 Heliophysics Connection

765

766 Missions to explore the Ice Giant Systems also resonate with the heliophysics community, as detailed
767 exploration of an oblique rotator can inform a universal model of magnetospheres. The panel on solar-wind
768 magnetosphere interactions of the 2013 heliophysics decadal survey⁵ identified how the magnetospheres of
769 Uranus and Neptune are fundamentally different from others in our Solar System, and sought to ensure that
770 magnetic field instruments would be guaranteed a place on outer planet missions, with a strong
771 recommendation being that NASA's heliophysics and planetary divisions partner on a Uranus orbital mission.
772 They describe how Uranus offers an example of solar wind/magnetosphere interactions under strongly
773 changing orientations over diurnal timescales. Depending on the season, the effects of solar wind-
774 magnetosphere interaction vary dramatically over the course of each day.

775

⁵ <https://www.nap.edu/catalog/13060/solar-and-space-physics-a-science-for-a-technological-society>

776 There is also a need to understand how the solar wind evolves beyond 10 AU (Saturn orbit), as the states of
777 solar structures travelling within the solar wind (solar wind pressure pulses) are largely unknown due to the
778 lack of observations at such large heliocentric distances (Witasse et al., 2017). The long cruise duration of a
779 mission to Uranus or Neptune provides an excellent opportunity for both heliophysics and Ice Giant
780 communities if a space weather-monitoring package that includes a magnetometer, a solar wind analyser,
781 and a radiation monitor operates continuously during the cruise phase, to understand how conditions vary
782 out to 20-30 AU over a prolonged lifetime. Moreover, the complexity of the interactions of Uranus's
783 magnetosphere with the solar wind provides an ideal testbed for the theoretical understanding of planetary
784 interactions with the solar wind, significantly expanding the parameter range over which scientists can study
785 magnetospheric structure and dynamics. The potential discoveries from its dynamo generation and its
786 variability stand to open new chapters in comparative planetary magnetospheres and interiors.

787

788 3.3 Exoplanet & Brown Dwarf Connection

789

790 The Ice Giant System mission will occur during an explosion in our understanding of planets beyond our Solar
791 System, through ESA's Cosmic Vision missions Plato, Euclid, and ARIEL; through missions with international
792 partners like JWST and TESS; and through next-generation observatories likeWFIRST, LUVOIR, Origins, and
793 HabEx. The physical and chemical processes at work within our own Solar System serve as the key foundation
794 for our understanding of those distant and unresolved worlds. Our Solar System provides the only laboratory
795 in which we can perform in-situ experiments to understand exoplanet formation, composition, structure,
796 dynamos, systems and magnetospheres. After the several highly-successful missions to the Gas Giants (and
797 the upcoming ESA/JUICE mission), dedicated exploration of the Ice Giants would place those discoveries into
798 a broader, solar-system context.

799

800 **Planet Statistics:** Uranus and Neptune represent our closest and best examples of a class of planets
801 intermediate in mass and size between the larger, hydrogen-helium-enriched gas giants, and the rocky

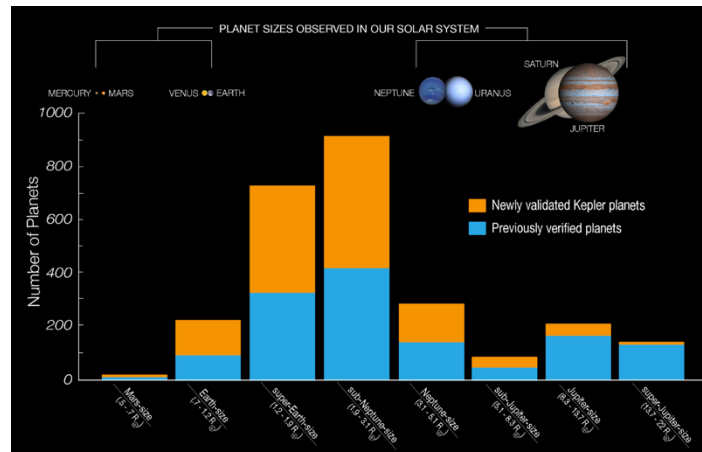


Figure 7 Known transiting exoplanets in 2016, from the Kepler mission, showing sub-Neptunes as the most common planetary radius in the current census. Credit: NASA/Ames

802 terrestrial worlds. Indeed, Neptune- and sub-Neptune-size worlds have emerged as commonplace in our
 803 ever-expanding census of exoplanets (Figure 7). Neptune-size planets are among the most common classes
 804 of exoplanet in our galaxy (Fulton et al., 2018). Fressin et al. (2013) suggest that this category of planets can
 805 be found around 3-31% of sun-like stars, and Petigura et al (2017) suggests that sub-Neptunes remains the
 806 most common category within Kepler's survey. Based on statistics from the Kepler mission it is predicted that
 807 TESS will detect over 1500 sub-Neptunes ($2-4 R_E$) over the mission (Barclay et al. 2018). Microlensing surveys
 808 (e.g., WFIRST, Penny et al., 2019) will also be more sensitive to lower-mass planets on wide orbits, and could
 809 reveal new insights into extrasolar Ice Giants ahead of a mission to Uranus or Neptune. Given these planetary
 810 occurrence rates, the exploration of bulk composition and interiors of our Ice Giants would provide strong
 811 constraints on the most common outcome for planetary formation. However, we emphasise that being
 812 Neptune-sized does not necessarily imply being Neptune-like, as a plethora of additional parameters come
 813 into play to shape the environmental conditions on these worlds.

814

815 **Atmospheric Insights:** Although we are currently unable to resolve spatial contrasts on exoplanets and brown
 816 dwarfs, comparisons of dayside (eclipse) and nightside (transit) spectra suggest the presence of powerful
 817 winds on some targets that are responsible for redistribution of energy. Brightness variations as Brown
 818 Dwarfs rotate suggest patchy cloud structures, but their rapid evolution was only understood when
 819 compared with long-cadence Neptune observations (Apai et al., 2013, Stauffer et al. 2016, Simon et al. 2016).
 820 Changes in exoplanet transit spectra with temperature indicate complex cloud condensation processes

821 (Morley et al., 2012; Wakeford et al., 2017). Atmospheric dynamics, chemistry, and cloud formation all vary
822 as a function of planetary age, distance from the host star, and the bulk enrichments of chemical species.
823 The smaller radii of Uranus and Neptune, compared to the larger gas giants, implies atmospheric processes
824 (zonal banding, storms, vortices) at work in a different region of dynamical parameter space, and one which
825 is unavailable elsewhere in our Solar System. Detailed exploration of our Ice Giants, in comparison to the
826 existing studies of the Gas Giants, would allow us to unravel these competing and complex phenomena
827 shaping the atmospheres of exoplanets and brown dwarfs. Importantly, measurements of Ice Giant
828 composition and dynamics can be directly compared to exoplanet and brown dwarf observations, placing
829 their formation location, age, and evolution into context, and vice versa. However, this cannot be done
830 without a detailed comparative dataset from our Solar System Ice Giants.

831

832 **Magnetospheric Insights:** Rymer et al. (2018) explore the importance of Ice Giant interactions with the wider
833 magnetic environment as a testbed for understanding exoplanets. Eccentric and complex orbital
834 characteristics appear commonplace beyond our Solar System, and Uranus is one of the only places where
835 radio emission, magnetospheric transport and diffusion resulting from a complex magnetospheric
836 orientation can be explored. The stability and strength of the Uranian radiation belts could also guide the
837 search for exoplanets with radiation belts. Finally, understanding the dynamos of Uranus and Neptune would
838 drastically improve our predictions of magnetic field strengths and exoplanet dynamo morphologies. Each
839 of these insights will be vital as exoplanetary science moves into an era of characterisation of atmospheric
840 composition, dynamics, clouds, and auroral/radio emissions.

841 4. Ice Giant Missions

842 4.1 Architectures: The Case for Orbiters

843

844 The scientific themes of Ice Giant System missions (summarised in Figure 9) are broad and challenging to
845 capture within a single mission architecture, but recent efforts by both ESA (e.g., the 2018-19 studies with

846 the Concurrent Design Facility for an M*-class mission⁶) and NASA (e.g., the 2017 Science Study Team report,
847 Hofstadter et al., 2019)⁷ have explored strategies to achieve many of the goals in Section 2. The joint NASA-
848 ESA science study team provided a detailed investigation of various combinations of flyby missions, orbiters,
849 multiple sub-satellites from a core spacecraft, satellite landers, and atmospheric probes. Strategies to
850 explore both Ice Giants with dual spacecraft have also been proposed (Turrini et al., 2014; Simon et al., 2018).
851 It was widely recognised that a flyby mission like Voyager, without any additional components like an entry
852 probe, was deemed to provide the lowest science return for the Ice Giants themselves, despite their lower
853 cost point. Without *in situ* measurements, and by providing only brief snapshots of the evolving atmospheres
854 and magnetospheres, and limited coverage of the satellites and rings, a flyby could not deliver on the highest-
855 priority science goals for an Ice Giant mission. Targeting Triton as a flyby, or the inclusion of an entry probe,
856 would increase the scientific reach, but would still prove inadequate for whole-system science. The study
857 found that an Ice Giant orbiter, to either Uranus or Neptune, would provide an unprecedented leap in our
858 understanding of these enigmatic worlds. An orbiter would maximise the time spent in the system to conduct
859 science of interest to the entire planetary community.

860

861 In our 2019 submission to ESA's call for ideas to shape the planning of space science missions in the coming
862 decades (known as Voyage 2050), we therefore proposed that an orbital mission to an Ice Giant should be
863 considered as a cornerstone of ESA's Voyage 2050 programme, if not already initiated with our international
864 partners in the coming decade. An ESA orbital mission, powered by radioisotope thermoelectric generators,
865 should be studied as an L-class mission to capitalise on the wealth of European experience of the Cassini and
866 JUICE missions. Alternatively, an M-class Ice Giant budget would allow a crucial contribution to an orbital
867 mission led by our international partners. The mass and mission requirements associated with additional
868 components, such as satellite landers, *in situ* probes, or secondary small satellites, must be tensioned against

⁶ <http://sci.esa.int/future-missions-department/61307-cdf-study-report-ice-giants/>

⁷ <https://www.lpi.usra.edu/icegiants/>

869 the capabilities of the core payload, and the capability of the launch vehicle and propulsion. In all of these
870 cases, a formal study of the requirements and capabilities is necessary to mature the concept.

871

872 **Payload Considerations:** The 2017 NASA study found that payload masses of 90-150 kg could deliver
873 significant scientific return for a flagship-class mission, whilst the 2018 ESA CDF study identified 100 kg as a
874 realistic payload mass for a European orbiter. Different studies have resulted in different prioritisations for
875 instrumentation, but produced suites of orbiter experiments in common categories. Multi-spectral remote
876 sensing is required, using both imaging and spectroscopy, spanning the UV, visible, near-IR (e.g.,
877 atmosphere/surface reflectivity, dynamics; auroral observations), mid-IR, sub-mm, to centimetre
878 wavelengths (e.g., thermal emission and energy balance, atmospheric circulation). Such remote sensing is
879 also a requirement for characterising any atmospheric probe entry sites, or satellite lander sites. Direct
880 sensing of the magnetospheric and plasma environment would be accomplished via magnetometers, dust
881 detectors, plasma instruments, radio wave detectors, and potentially mass spectrometers. Radio science
882 would provide opportunities for interior sounding and neutral/ionospheric occultation studies. The provision
883 of such instruments would capitalise on European heritage on Cassini, JUICE, Rosetta, Venus/Mars Express,
884 and Bepi Colombo, but at the same time recognising the need to develop smaller, lighter, and less
885 power/data-intensive instruments, raising and maturing their technological readiness.

886

887 **Orbit Considerations:** Orbital missions to both Uranus and Neptune depend crucially on the chemical fuel
888 required for orbit insertion, which determines the deliverable mass. The potential use of aerocapture, using
889 atmospheric drag to slow down the spacecraft, permits larger payloads and faster trip times at the expense
890 of increased risk, which needs significant further study. Mission requirements and orbital geometries will
891 determine the inclination of orbital insertion – high geographical latitudes would benefit some atmospheric,
892 rings, and magnetospheric science, but satellite gravity assists and subsequent trajectory corrections would
893 be needed for exploration of the satellites, rings and atmosphere from a low-inclination orbit. High
894 inclinations are easier to achieve at Uranus, although Triton can be used to drive a satellite tour at Neptune.

895 We also propose that distinct phases of an orbital tour be considered, balancing moderate orbital distances
896 (for remote sensing, outer magnetosphere science, and a satellite tour) with close-in final orbits (for gravity
897 science and inner magnetosphere), following the example of Cassini and Juno. Multiple close flybys of major
898 satellites are desirable to map their interiors, surfaces, and atmospheres via a variety of techniques. Finally,
899 multi-year orbital tours (at least \sim 3 years) would maximise our time in the system, permitting the study of
900 atmospheric and magnetospheric changes over longer time periods. The 2018 ESA CDF study confirmed the
901 feasibility of orbital tours satisfying these scientific requirements.

902

903 **Ring Hazards:** The 2017 NASA-ESA report highlighted potentially unknown ring-plane hazards as a topic for
904 future study. Orbit insertion should be as close to the planet as possible to reduce the required fuel, but the
905 properties of Ice Giant rings remain poorly constrained. Potential options to mitigate this risk include: having
906 the insertion be further out (requiring more fuel); fly through the ring plane at an altitude where atmospheric
907 drag is high enough to reduce the number of particles, but not enough to adversely affect the spacecraft; use
908 a pathfinder spacecraft to measure the particle density ahead of time; or use Earth-based observations to
909 constrain the upper atmosphere/ring hazard. Detailed calculations on the location of this safe zone are
910 required.

911

912 4.2 Timeliness and Launch Opportunities

913

914 Trajectories to reach the Ice Giants depend on a number of factors: the use of chemical and/or solar-electric
915 propulsion (SEP) technologies; the lift capacity of the launch vehicle; the use of aerocapture/aerobraking;
916 and the need for gravity assists. The availability of Jupiter, as the largest planet, is key to optimal launch
917 trajectories, and the early 2030s offer the best opportunities. The synodic periods of Uranus and Neptune
918 with respect to Jupiter are \sim 13.8 and \sim 12.8 years, respectively, meaning that optimal Jupiter gravity-assist
919 (GA) windows occur every 13-14 years. The NASA-ESA joint study team identified chemical-propulsion
920 opportunities with a Jupiter GA in 2029-30 for Neptune, and a wider window of 2030-34 for Uranus. Such

921 windows would repeat in the 2040s, and a wider trade space (including the potential to use Saturn GA) should
922 be explored. We stress that a mission to an Ice Giant is feasible using conventional chemical propulsion.

923

924 Furthermore, a mission launched to Uranus or Neptune could offer significant opportunities for flybys of
925 Solar System objects en route, especially Centaurs, which are small bodies that orbit in the giant planet
926 region. This population has yet to be explored by spacecraft, but represents an important evolutionary step
927 between Kuiper Belt objects and comets. Around 300 are currently known, with 10% of these observed to
928 show cometary activity. In addition, we can expect to discover at least an order of magnitude more Centaurs
929 by the 2030s, following discoveries by the Large Synoptic Survey Telescope, increasing the probability that a
930 suitable flyby target can be found near to the trajectory to Uranus/Neptune. Some of the largest of the
931 Centaurs (~100 km scale objects) have their own ring systems, the origin of which has yet to be explained,
932 while smaller ones (1-10 km scale) could add an important ‘pre-activity’ view to better interpret data from
933 Rosetta’s exploration of a comet. The payload options described in Section 4 would be well suited to
934 characterise a Centaur during a flyby.

935

936 The launch time necessarily influences the arrival time, as depicted in Figure 8. Uranus will reach northern
937 summer solstice in 2030, and northern autumnal equinox in 2050. Voyager 2 observed near northern winter
938 solstice, meaning that the north poles of the planet and satellites were shrouded in darkness. These
939 completely unexplored northern terrains will begin to disappear into darkness again in 2050, where they will
940 remain hidden for the following 42 years (half a Uranian year).

941

942 Neptune passed northern winter solstice in 2005, and will reach northern spring equinox in 2046. After this
943 time, the southern hemispheres of the planet and satellites (most notably the plumes of Triton at high
944 southern latitudes) will sink into winter darkness, meaning that the Triton plumes – if they are indeed
945 restricted to the south – would no longer be in sunlight after ~2046, and would remain hidden for the next
946 ~82 years (half a Neptunian year).

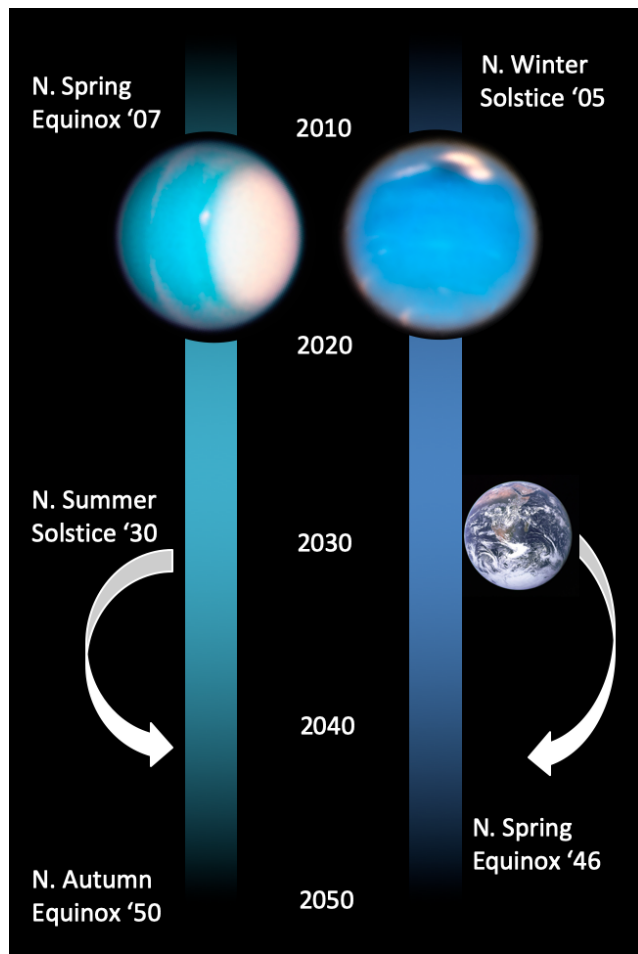


Figure 8 Potential timeline of missions to Uranus (left) and Neptune (right), compared to the seasons on each Ice Giant. The white arrows show the approximate timescales for launch opportunities in the early 2030s, with arrival in the 2040s.

947

948 The 2028-34 launch opportunities were assessed by the joint ESA-NASA study team. Saturn GA was
949 considered but did not appear optimal for this launch window. Interplanetary flight times are 6 to 12 years
950 to Uranus, 8 to 13 years to Neptune, depending on launch year, mission architecture, and launch vehicle.
951 The greater challenge of reaching the Neptune system was reflected in their choice of detailed architecture
952 studies: five missions to Uranus (orbiters with/without probes; with/without SEP; and with different payload
953 masses), and a single orbiter and probe for Neptune. Both Uranus and Neptune were deemed equally
954 valuable as targets – Uranus standing out for its uniqueness; Neptune for the prospects of exploring Triton.
955 The choice between these two enticing destinations will ultimately be driven by launch opportunities and
956 deliverable mass to the systems.

957

958 We must capitalise on the current momentum within Europe, alongside our international partners, to make
959 use of the launch opportunities in the ~2030s. Such a mission would arrive at Uranus while we can still see
960 the totally-unexplored northern terrains, or at Neptune while we can still see the active geology of Triton.
961 Operations in the 2040s would also allow ESA to maintain Outer Solar System expertise from current and
962 future missions like JUICE. An Ice Giant explorer would therefore be active as a cornerstone of ESA's Voyage
963 2050 strategic planning for space missions.

964

965 4.3 Mature and Developing Technologies

966

967 An ambitious mission to an Ice Giant System would largely build on existing mature technologies (e.g., see
968 the discussion of payload development in Section 4.1), but several challenges have been identified that, if
969 overcome, would optimise and enhance our first dedicated orbital mission to these worlds. Note that we
970 omit the need for ablative materials on atmospheric entry probes, which will be required for *in situ* science
971 (Mousis et al., 2018). Key areas where technology maturations are required include:

972

973 **Space nuclear power:** With the prospect of flying solar-powered spacecraft to 20 AU being non-viable, an
974 Ice Giant System mission must rely on radioisotope power sources, both for electricity and for spacecraft
975 heating. In the US, existing MMRTGs (multi-mission radioisotope thermal generators), based on the decay of
976 ^{238}Pu , will be re-designed to create eMMRTGs (“enhanced”) to increase the available specific power at the
977 end of life, 4-5 of which were considered for the mission architectures studied in the 2017 NASA-ESA report.
978 Previous M-class Uranus mission proposals have relied on US provision of these power sources for an ESA-
979 led mission. However, ESA continues to pursue the development of independent power sources based on
980 ^{241}Am . Whilst the power density is lower than that of ^{238}Pu , the half-life is much longer, and much of the
981 material is available from the reprocessing of spent fuel from European nuclear reactors, extracted
982 chemically from plutonium to a ceramic oxide form. Prototypes for both radioisotope heater units (warming
983 the spacecraft) and thermoelectric generators (providing spacecraft power) have now been demonstrated,

984 and development is continuing for operational use late in the next decade. An Ice Giant System mission could
985 benefit tremendously from this independent European power source.

986

987 **Hardware longevity:** Given the 6-13-year interplanetary transfer, coupled with the desire for a long orbital
988 tour, Ice Giant orbiters must be designed to last for a long duration under a variable thermal load imposed
989 by gravity assists from the inner to the outer solar system. This poses constraints on the reliability of parts
990 and power sources, as well as the need to develop optimised operational plans for the long cruise phases,
991 such as the use of hibernation modes following the example of New Horizons.

992

993 **Telemetry/Communications:** All missions to the giant planets are somewhat constrained by the reduced
994 data rates at large distances from Earth, but the case at Uranus and Neptune is most severe. With current
995 ESA ground-stations, the science tours would need optimisation to allow for long periods of data downlink,
996 with implications for the available power on the spacecraft. European development or access to US 70-m
997 Deep Space Network capabilities with state-of-the-art Ka-band technology would greatly improve the
998 situation, but even here the bandwidth would remain small. We would welcome detailed studies of new
999 communications technologies, such as optical communications, as a general enabling technology for solar
1000 system exploration. However, we recognise that achieving the required directionality of a downlink laser
1001 from beyond 5AU will be challenging. Nevertheless, the 2018 ESA CDF study confirmed that the data volume
1002 of a realistic M-class mission scenario to Uranus could be downlinked to Earth even with current
1003 technologies. In the case of Neptune, some data optimization strategy would be required.

1004

1005 **Electromagnetic cleanliness:** A number of the proposed payload elements (magnetometers, plasma and
1006 radio instruments) impose strict EMC requirements on the spacecraft, and new technologies and cost
1007 optimisation strategies should be explored to reduce these EMC issues.

1008

1009 **Launch Vehicles:** The market for launch vehicles is changing dramatically both in Europe and in the US, but
1010 an Ice Giant System cornerstone mission could take advantage of the latest technologies, delivering as much
1011 mass to the system as possible within the constraints of a realistic flight time. Larger launch vehicles may
1012 also open up the prospect for multiple spacecraft to share the same fairing.

1013 5. Summary and Perspectives

1014

1015 This article reviews and updates the scientific rationale for a mission to an Ice Giant system, advocating that
1016 an orbital mission (alongside an atmospheric entry probe) be considered as a cornerstone of ESA's Voyage
1017 2050 programme, working in collaboration with international partners to launch the ***first dedicated mission***
1018 to either Uranus or Neptune. Using technologies both mature and in development, the Ice Giants community
1019 hopes to capitalise on launch opportunities in the 2030s to reach the Ice Giants. As shown in Figure 9, an Ice
1020 Giant System mission would engage a wide community, drawing expertise from a vast range of disciplines
1021 *within* planetary science, from surface geology to planetary interiors; from meteorology to ionospheric
1022 physics; from plasma scientists to heliophysicists. But this challenge is also interdisciplinary in nature,
1023 engaging those studying potentially similar Neptune-size objects beyond our Solar System, by revealing the
1024 properties of this underexplored class of planetary objects. As Neptune's orbit shapes the dynamical
1025 properties of objects in the distant solar system, an Ice Giant System mission also draws in the small-bodies
1026 community investigating objects throughout the Outer Solar System, from Centaurs, to TNOs, to Kuiper Belt
1027 Objects, and contrasting these with the natural satellites of Uranus.

1028

1029 To launch a mission to Uranus and/or Neptune in the early 2030s, the international Ice Giant community
1030 needs to significantly raise the maturity of the mission concepts and instrument technological readiness. At
1031 the time of writing (late 2019), we await the outcomes of both ESA's Voyage 2050 process, and the next US
1032 planetary decadal survey. Nevertheless, this should not delay the start of a formal science definition and
1033 study process (pre-phase A conceptual studies), so that we are ready to capitalise on any opportunities that
1034 these strategic planning surveys provide. Fully costed and technologically robust mission concepts need to

1035 be developed, studied, and ready for implementation by 2023-25 to have the potential to meet the upcoming
1036 window for Jupiter gravity assists between 2029-2034. We hope that the scientific themes and rationale
1037 identified in this review will help to guide that conceptual study process, to develop a paradigm-shifting
1038 mission that will help redefine planetary science for a generation of scientists and engineers.

1039

1040 Most importantly, the Ice Giant System mission will continue the breath-taking legacy of discovery of the
1041 Voyager, Galileo, Cassini, Juno and JUICE missions to the giant planets. A dedicated orbiter of an Ice Giant is
1042 the next logical step in our exploration of the Solar System, completing humankind's first reconnaissance of
1043 the eight planets. It will be those discoveries that no one expected, those mysteries that we did not
1044 anticipate, and those views that no human has previously witnessed, which will enthuse the general public,
1045 and inspire the next generation of explorers to look to the worlds of our Solar System. We urge both ESA
1046 and NASA to take up this challenge.

1047

1048

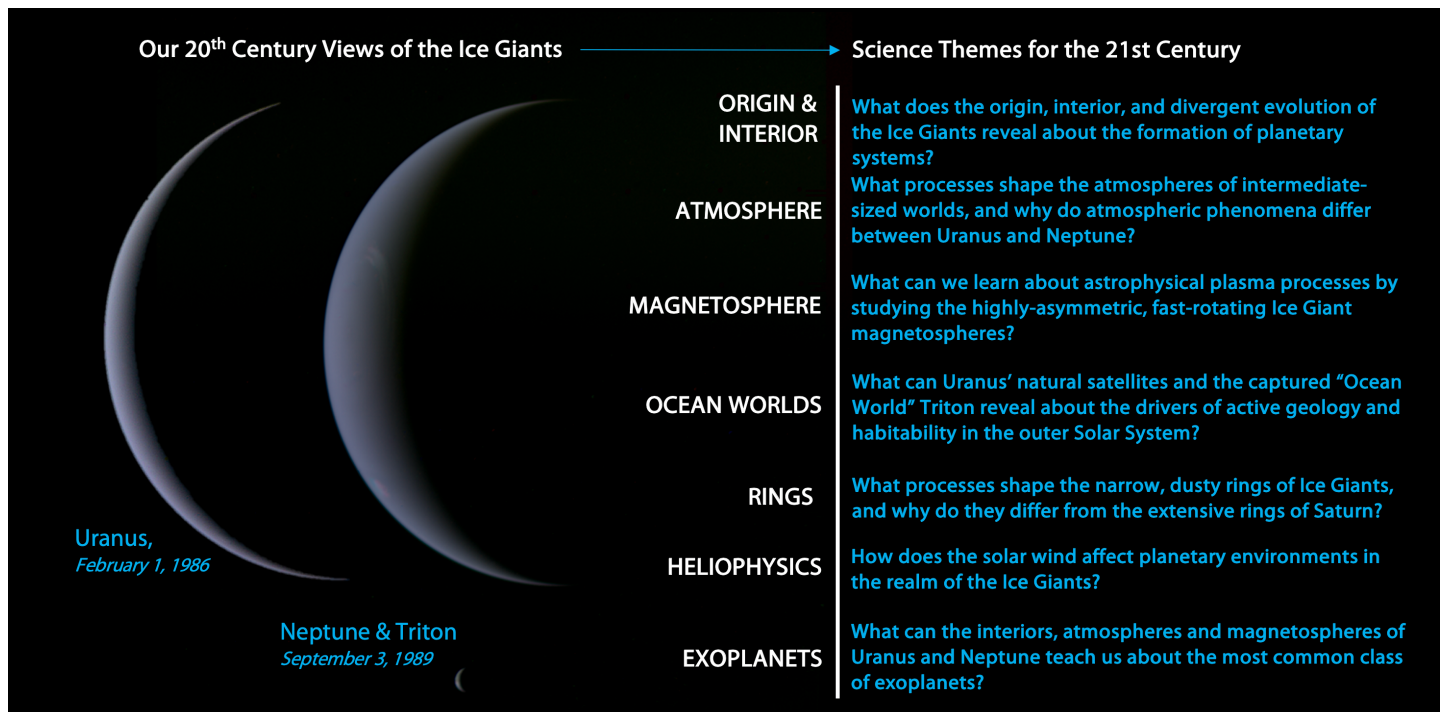


Figure 9 Left: Our last views of Uranus and Neptune from a robotic spacecraft, taken by Voyager 2 three decades ago (Credit: NASA/JPL/E. Lakdawalla). Will we see these views again before a half-century has elapsed? Right: Seven science themes for Voyage 2050 that could be addressed by an Ice Giant System mission.

1049

1050 Acknowledgements

1051

1052 Fletcher was supported by a Royal Society Research Fellowship and European Research Council Consolidator
 1053 Grant (under the European Union's Horizon 2020 research and innovation programme, grant agreement No
 1054 723890) at the University of Leicester. Mousis acknowledges support from CNES. Hueso was supported by
 1055 the Spanish MINECO project AYA2015-65041-P (MINECO/FEDER, UE) and by Grupos Gobierno Vasco IT1366-
 1056 19 from Gobierno Vasco. UK authors acknowledge support from the Science and Technology Facilities
 1057 Council (STFC). The authors are grateful to Beatriz Sanchez-Cano, Colin Snodgrass, Hannah Wakeford,
 1058 Marius Millot, and Radek Poleski for their comments on early drafts of this article. We are grateful to the
 1059 members of ESA's Voyage 2050 Senior Committee for allowing us to present this review at the Voyage 2050
 1060 workshop in Madrid in October 2019 (see <https://www.cosmos.esa.int/web/voyage-2050/workshop-programme>).
 1061

1062

1063 References

1064

1065 Apai, D., Radigan, J., Buenzli, E., Burrows, A., Reid, I. N., & Jayawardhana, R. (2013), HST Spectral Mapping of
1066 L/T Transition Brown Dwarfs Reveals Cloud Thickness Variations, *The Astrophysical Journal*, 768, 121,
1067 10.1088/0004-637X/768/2/121.

1068

1069 Arridge, C. S., Achilleos, N., Agarwal, J., Agnor, C. B., Ambrosi, R., André, N., Badman, S. V., Baines, K., Banfield,
1070 D., et al. (2014), The science case for an orbital mission to Uranus: Exploring the origins and evolution of ice
1071 giant planets, *Planetary and Space Science*, 104, 122, 10.1016/j.pss.2014.08.009.

1072

1073 Arridge, C. S., Agnor, C. B., André, N., Baines, K. H., Fletcher, L. N., Gautier, D., Hofstadter, M. D., Jones, G. H.,
1074 Lamy, L., et al. (2012), Uranus Pathfinder: exploring the origins and evolution of Ice Giant planets,
1075 *Experimental Astronomy*, 33, 753, 10.1007/s10686-011-9251-4.

1076

1077 Bailey, E., & Stevenson, D. J. (2015), Modeling Ice Giant Interiors Using Constraints on the H₂-H₂O Critical
1078 Curve, *AGU Fall Meeting Abstracts*, 2015, P31G-03,.

1079

1080 Bali, E., Audétat, A., & Keppler, H. (2013), Water and hydrogen are immiscible in Earth's mantle, *Nature*, 495,
1081 220, 10.1038/nature11908.

1082

1083 Barclay, T., Pepper, J., & Quintana, E. V. (2018), A Revised Exoplanet Yield from the Transiting Exoplanet
1084 Survey Satellite (TESS), *The Astrophysical Journal Supplement Series*, 239, 2, 10.3847/1538-4365/aae3e9.

1085

1086 Barthélémy, M., Lamy, L., Menager, H., Schulik, M., Bernard, D., Abgrall, H., Roueff, E., Cessateur, G., Prange,
1087 R., et al. (2014), Dayglow and auroral emissions of Uranus in H₂ FUV bands, *Icarus*, 239, 160,
1088 10.1016/j.icarus.2014.05.035.

1089

1090 Batalha, N. M., Rowe, J. F., Bryson, S. T., Barclay, T., Burke, C. J., Caldwell, D. A., Christiansen, J. L., Mullally,
1091 F., Thompson, S. E., et al. (2013), Planetary Candidates Observed by Kepler. III. Analysis of the First 16 Months
1092 of Data, *The Astrophysical Journal Supplement Series*, 204, 24, 10.1088/0067-0049/204/2/24.

1093

1094 Boué, G., & Laskar, J. (2010), A Collisionless Scenario for Uranus Tilting, *The Astrophysical Journal*, 712, L44,
1095 10.1088/2041-8205/712/1/L44.

1096

1097 Broadfoot, A. L., Herbert, F., Holberg, J. B., Hunten, D. M., Kumar, S., Sandel, B. R., Shemansky, D. E., Smith,
1098 G. R., Yelle, R. V., et al. (1986), Ultraviolet Spectrometer Observations of Uranus, *Science*, 233, 74,
1099 10.1126/science.233.4759.74.

1100

1101 Broadfoot, A. L., Atreya, S. K., Bertaux, J. L., Blamont, J. E., Dessler, A. J., Donahue, T. M., Forrester, W. T.,
1102 Hall, D. T., Herbert, F., et al. (1989), Ultraviolet Spectrometer Observations of Neptune and Triton, *Science*,
1103 246, 1459, 10.1126/science.246.4936.1459.

1104

1105 Brown, R. H., & Cruikshank, D. P. (1983), The Uranian satellites: Surface compositions and opposition
1106 brightness surges, *Icarus*, 55, 83, 10.1016/0019-1035(83)90052-0.

1107

1108 Buchvarova, M., & Velinov, P. (2009), Cosmic ray spectra in planetary atmospheres, *Universal Heliophysical
1109 Processes*, 257, 471, 10.1017/S1743921309029718.

1110

1111 Běhouková, M., Tobie, G., Choblet, G., & Čadek, O. (2012), Tidally-induced melting events as the origin of
1112 south-pole activity on Enceladus, *Icarus*, 219, 655, 10.1016/j.icarus.2012.03.024.

1113

- 1114 Cao, X., & Paty, C. (2017), Diurnal and seasonal variability of Uranus's magnetosphere, *Journal of Geophysical*
1115 *Research (Space Physics)*, 122, 6318, 10.1002/2017JA024063.
- 1116
- 1117 Cartwright, R. J., Emery, J. P., Rivkin, A. S., Trilling, D. E., & Pinilla-Alonso, N. (2015), Distribution of CO₂ ice
1118 on the large moons of Uranus and evidence for compositional stratification of their near-surfaces, *Icarus*,
1119 257, 428, 10.1016/j.icarus.2015.05.020.
- 1120
- 1121 Cartwright, R. J., Emery, J. P., Pinilla-Alonso, N., Lucas, M. P., Rivkin, A. S., & Trilling, D. E. (2018), Red material
1122 on the large moons of Uranus: Dust from the irregular satellites?, *Icarus*, 314, 210,
1123 10.1016/j.icarus.2018.06.004.
- 1124
- 1125 Cavalié, T., Venot, O., Selsis, F., Hersant, F., Hartogh, P., & Leconte, J. (2017), Thermochemistry and vertical
1126 mixing in the tropospheres of Uranus and Neptune: How convection inhibition can affect the derivation of
1127 deep oxygen abundances, *Icarus*, 291, 1, 10.1016/j.icarus.2017.03.015.
- 1128
- 1129 Christophe, B., Spilker, L. J., Anderson, J. D., André, N., Asmar, S. W., Aurnou, J., Banfield, D., Barucci, A.,
1130 Bertolami, O., et al. (2012), OSS (Outer Solar System): a fundamental and planetary physics mission to
1131 Neptune, Triton and the Kuiper Belt, *Experimental Astronomy*, 34, 203, 10.1007/s10686-012-9309-y.
- 1132
- 1133 Colwell, J. E., & Esposito, L. W. (1993), Origins of the rings of Uranus and Neptune. 2. Initial conditions and
1134 ring moon populations, *Journal of Geophysical Research*, 98, 7387, 10.1029/93JE00329.
- 1135
- 1136 Colwell, J. E., & Esposito, L. W. (1992), Origins of the rings of Uranus and Neptune 1. Statistics of satellite
1137 disruptions, *Journal of Geophysical Research*, 97, 10227, 10.1029/92JE00788.
- 1138

- 1139 Conrath, B. J., Gierasch, P. J., & Ustinov, E. A. (1998), Thermal Structure and Para Hydrogen Fraction on the
1140 Outer Planets from Voyager IRIS Measurements, *Icarus*, 135, 501, 10.1006/icar.1998.6000.
- 1141
- 1142 Cowley, S. W. H. (2013), Response of Uranus' auroras to solar wind compressions at equinox, *Journal of*
1143 *Geophysical Research (Space Physics)*, 118, 2897, 10.1002/jgra.50323.
- 1144
- 1145 Croft, S. K., & Soderblom, L. A. (1991), Geology of the Uranian satellites., *Uranus*, 561,.
- 1146
- 1147 Cruikshank, D. P., Schmitt, B., Roush, T. L., Owen, T. C., Quirico, E., Geballe, T. R., de Bergh, C., Bartholomew,
1148 M. J., Dalle Ore, C. M., et al. (2000), Water Ice on Triton, *Icarus*, 147, 309, 10.1006/icar.2000.6451.
- 1149
- 1150 de Pater, I., Hammel, H. B., Showalter, M. R., & van Dam, M. A. (2007), The Dark Side of the Rings of Uranus,
1151 *Science*, 317, 1888, 10.1126/science.1148103.
- 1152
- 1153 de Pater, I., Gibbard, S. G., & Hammel, H. B. (2006), Evolution of the dusty rings of Uranus, *Icarus*, 180, 186,
1154 10.1016/j.icarus.2005.08.011.
- 1155
- 1156 de Pater, I., Gibbard, S. G., Chiang, E., Hammel, H. B., Macintosh, B., Marchis, F., Martin, S. C., Roe, H. G., &
1157 Showalter, M. (2005), The dynamic neptunian ring arcs: evidence for a gradual disappearance of Liberté and
1158 resonant jump of courage, *Icarus*, 174, 263, 10.1016/j.icarus.2004.10.020.
- 1159
- 1160 de Pater, I., Romani, P. N., & Atreya, S. K. (1991), Possible microwave absorption by H₂S gas in Uranus' and
1161 Neptune's atmospheres, *Icarus*, 91, 220, 10.1016/0019-1035(91)90020-T.
- 1162

- 1163 de Pater, I., Fletcher, L. N., Luszcz-Cook, S., DeBoer, D., Butler, B., Hammel, H. B., Sitko, M. L., Orton, G., &
1164 Marcus, P. S. (2014), Neptune's global circulation deduced from multi-wavelength observations, *Icarus*, 237,
1165 211, 10.1016/j.icarus.2014.02.030.
- 1166
- 1167 de Pater, I., Sromovsky, L. A., Fry, P. M., Hammel, H. B., Baranec, C., & Sayanagi, K. M. (2015), Record-breaking
1168 storm activity on Uranus in 2014, *Icarus*, 252, 121, 10.1016/j.icarus.2014.12.037.
- 1169
- 1170 Decker, R. B., & Cheng, A. F. (1994), A model of Triton's role in Neptune's magnetosphere, *Journal of
1171 Geophysical Research*, 99, 19027, 10.1029/94JE01867.
- 1172
- 1173 Dodson-Robinson, S. E., & Bodenheimer, P. (2010), The formation of Uranus and Neptune in solid-rich feeding
1174 zones: Connecting chemistry and dynamics, *Icarus*, 207, 491, 10.1016/j.icarus.2009.11.021.
- 1175
- 1176 Dumas, C., Terrile, R. J., Smith, B. A., Schneider, G., & Becklin, E. E. (1999), Stability of Neptune's ring arcs in
1177 question, *Nature*, 400, 733, 10.1038/23414.
- 1178
- 1179 Farrell, W. M. (1992), Nonthermal radio emissions from Uranus, *Planetary Radio Emissions III*, 241.,
- 1180
- 1181 Feuchtgruber, H., Lellouch, E., de Graauw, T., Bézard, B., Encrenaz, T., & Griffin, M. (1997), External supply of
1182 oxygen to the atmospheres of the giant planets, *Nature*, 389, 159, 10.1038/38236.
- 1183
- 1184 Fletcher, L. N., de Pater, I., Orton, G. S., Hammel, H. B., Sitko, M. L., & Irwin, P. G. J. (2014), Neptune at summer
1185 solstice: Zonal mean temperatures from ground-based observations, 2003-2007, *Icarus*, 231, 146,
1186 10.1016/j.icarus.2013.11.035.
- 1187

- 1188 French, R. G., Nicholson, P. D., Porco, C. C., & Marouf, E. A. (1991), Dynamics and structure of the Uranian
1189 rings., *Uranus*, 327,.
- 1190
- 1191 Fressin, F., Torres, G., Charbonneau, D., Bryson, S. T., Christiansen, J., Dressing, C. D., Jenkins, J. M.,
1192 Walkowicz, L. M., & Batalha, N. M. (2013), The False Positive Rate of Kepler and the Occurrence of Planets,
1193 *The Astrophysical Journal*, 766, 81, 10.1088/0004-637X/766/2/81.
- 1194
- 1195 Fulton, B. J., & Petigura, E. A. (2018), The California-Kepler Survey. VII. Precise Planet Radii Leveraging Gaia
1196 DR2 Reveal the Stellar Mass Dependence of the Planet Radius Gap, *The Astronomical Journal*, 156, 264,
1197 10.3847/1538-3881/aae828.
- 1198
- 1199 Gierasch, P. J., & Conrath, B. J. (1987), Vertical temperature gradients on Uranus: Implications for layered
1200 convection, *Journal of Geophysical Research*, 92, 15019, 10.1029/JA092iA13p15019.
- 1201
- 1202 Griton, L., Pantellini, F., & Meliani, Z. (2018), Three-Dimensional Magnetohydrodynamic Simulations of the
1203 Solar Wind Interaction With a Hyperfast-Rotating Uranus, *Journal of Geophysical Research (Space Physics)*,
1204 123, 5394, 10.1029/2018JA025331.
- 1205
- 1206 Griton, L. & Pantellini, F. (2020), Magnetohydrodynamic simulations of a Uranus-at-equinox type rotating
1207 magnetosphere, *Astronomy and Astrophysics*, 10.1051/0004-6361/201936604.
- 1208
- 1209 Grundy, W. M., Binzel, R. P., Buratti, B. J., Cook, J. C., Cruikshank, D. P., Dalle Ore, C. M., Earle, A. M., Ennico,
1210 K., Howett, C. J. A., et al. (2016), Surface compositions across Pluto and Charon, *Science*, 351, aad9189,
1211 10.1126/science.aad9189.
- 1212

- 1213 Grundy, W. M., Young, L. A., Spencer, J. R., Johnson, R. E., Young, E. F., & Buie, M. W. (2006), Distributions of
1214 H₂O and CO₂ ices on Ariel, Umbriel, Titania, and Oberon from IRTF/SpeX observations, *Icarus*, 184, 543,
1215 10.1016/j.icarus.2006.04.016.
- 1216
- 1217 Guillot, T. (1995), Condensation of Methane, Ammonia, and Water and the Inhibition of Convection in Giant
1218 Planets, *Science*, 269, 1697, 10.1126/science.7569896.
- 1219
- 1220 Gunell, H., Maggiolo, R., Nilsson, H., Stenberg Wieser, G., Slapak, R., Lindkvist, J., Hamrin, M., & De Keyser, J.
1221 (2018), Why an intrinsic magnetic field does not protect a planet against atmospheric escape, *Astronomy and
1222 Astrophysics*, 614, L3, 10.1051/0004-6361/201832934.
- 1223
- 1224 Gurnett, D. A., Kurth, W. S., Cairns, I. H., & Granroth, L. J. (1990), Whistlers in Neptune's magnetosphere:
1225 Evidence of atmospheric lightning, *Journal of Geophysical Research*, 95, 20967, 10.1029/JA095iA12p20967.
- 1226
- 1227 Helled, R., Bodenheimer, P., Podolak, M., Boley, A., Meru, F., Nayakshin, S., Fortney, J. J., Mayer, L., Alibert,
1228 Y., et al. (2014), Giant Planet Formation, Evolution, and Internal Structure, *Protostars and Planets VI*, 643,
1229 10.2458/azu_uapress_9780816531240-ch028.
- 1230
- 1231 Helled, R., Anderson, J. D., Podolak, M., & Schubert, G. (2011), Interior Models of Uranus and Neptune, *The
1232 Astrophysical Journal*, 726, 15, 10.1088/0004-637X/726/1/15.
- 1233
- 1234 Helled, R., Anderson, J. D., & Schubert, G. (2010), Uranus and Neptune: Shape and rotation, *Icarus*, 210, 446,
1235 10.1016/j.icarus.2010.06.037.
- 1236
- 1237 Helled, R., & Bodenheimer, P. (2014), The Formation of Uranus and Neptune: Challenges and Implications for
1238 Intermediate-mass Exoplanets, *The Astrophysical Journal*, 789, 69, 10.1088/0004-637X/789/1/69.

1239

1240 Helled, R. (2018), The Interiors of Jupiter and Saturn, Oxford Research Encyclopedia of Planetary Science,
1241 175, 10.1093/acrefore/9780190647926.013.175.

1242

1243 Helled, R., & Guillot, T. (2018), Internal Structure of Giant and Icy Planets: Importance of Heavy Elements and
1244 Mixing, *Handbook of Exoplanets*, 44, 10.1007/978-3-319-55333-7_44.

1245

1246 Herbert, F., Sandel, B. R., Yelle, R. V., Holberg, J. B., Broadfoot, A. L., Shemansky, D. E., Atreya, S. K., & Romani,
1247 P. N. (1987), The upper atmosphere of Uranus: EUV occultations observed by Voyager 2, *Journal of
1248 Geophysical Research*, 92, 15093, 10.1029/JA092iA13p15093.

1249

1250 Herbert, F. (2009), Aurora and magnetic field of Uranus, *Journal of Geophysical Research (Space Physics)*,
1251 114, A11206, 10.1029/2009JA014394.

1252

1253 Hofstadter, M., Simon, A., Atreya, S., Banfield, D., Fortney, J. J., Hayes, A., Hedman, M., Hospodarsky, G.,
1254 Mandt, K., et al. (2019), Uranus and Neptune missions: A study in advance of the next Planetary Science
1255 Decadal Survey, *Planetary and Space Science*, 177, 104680, 10.1016/j.pss.2019.06.004.

1256

1257 Hofstadter, M. D., & Butler, B. J. (2003), Seasonal change in the deep atmosphere of Uranus, *Icarus*, 165, 168,
1258 10.1016/S0019-1035(03)00174-X.

1259

1260 Hoogeveen, G. W., & Cloutier, P. A. (1996), The Triton-Neptune plasma interaction, *Journal of Geophysical
1261 Research*, 101, 19, 10.1029/95JA02761.

1262

- 1263 Hsu, H.-W., Schmidt, J., Kempf, S., Postberg, F., Moragas-Klostermeyer, G., Seiß, M., Hoffmann, H., Burton,
1264 M., Ye, S., et al. (2018), In situ collection of dust grains falling from Saturn's rings into its atmosphere, *Science*,
1265 362, aat3185, 10.1126/science.aat3185.
- 1266
- 1267 Hussmann, H., Sohl, F., & Spohn, T. (2006), Subsurface oceans and deep interiors of medium-sized outer
1268 planet satellites and large trans-neptunian objects, *Icarus*, 185, 258, 10.1016/j.icarus.2006.06.005.
- 1269
- 1270 Iess, L., Militzer, B., Kaspi, Y., Nicholson, P., Durante, D., Racioppa, P., Anabtawi, A., Galanti, E., Hubbard, W.,
1271 et al. (2019), Measurement and implications of Saturn's gravity field and ring mass, *Science*, 364, aat2965,
1272 10.1126/science.aat2965.
- 1273
- 1274 Irwin, P. G. J., Toledo, D., Garland, R., Teanby, N. A., Fletcher, L. N., Orton, G. A., & Bézard, B. (2018), Detection
1275 of hydrogen sulfide above the clouds in Uranus's atmosphere, *Nature Astronomy*, 2, 420, 10.1038/s41550-
1276 018-0432-1.
- 1277
- 1278 Jacobson, R. A. (2014), The Orbits of the Uranian Satellites and Rings, the Gravity Field of the Uranian System,
1279 and the Orientation of the Pole of Uranus, *The Astronomical Journal*, 148, 76, 10.1088/0004-6256/148/5/76.
- 1280
- 1281 Jacobson, R. A. (2009), The Orbits of the Neptunian Satellites and the Orientation of the Pole of Neptune,
1282 *The Astronomical Journal*, 137, 4322, 10.1088/0004-6256/137/5/4322.
- 1283
- 1284 Karkoschka, E., & Tomasko, M. G. (2011), The haze and methane distributions on Neptune from HST-STIS
1285 spectroscopy, *Icarus*, 211, 780, 10.1016/j.icarus.2010.08.013.
- 1286
- 1287 Kaspi, Y., Showman, A. P., Hubbard, W. B., Aharonson, O., & Helled, R. (2013), Atmospheric confinement of
1288 jet streams on Uranus and Neptune, *Nature*, 497, 344, 10.1038/nature12131.

1289

1290 Kegerreis, J. A., Eke, V. R., Gonnet, P., Korycansky, D. G., Massey, R. J., Schaller, M., & Teodoro, L. F. A. (2019),
1291 Planetary giant impacts: convergence of high-resolution simulations using efficient spherical initial conditions
1292 and SWIFT, *Monthly Notices of the Royal Astronomical Society*, 487, 5029, 10.1093/mnras/stz1606.

1293

1294 Kempf, S., Altobelli, N., Srama, R., Cuzzi, J., & Estrada, P. (2018), The Age of Saturn's Rings Constrained by the
1295 Meteoroid Flux Into the System, *EGU General Assembly Conference Abstracts*, 10791,.

1296

1297 Krasnopolsky, V. A., & Cruikshank, D. P. (1995), Photochemistry of Triton's atmosphere and ionosphere.,
1298 *Journal of Geophysical Research*, 100, 21,271,286,.

1299

1300 Lainey, V. (2008), A new dynamical model for the Uranian satellites, *Planetary and Space Science*, 56, 1766,
1301 10.1016/j.pss.2008.02.015.

1302

1303 Lambrechts, M., Johansen, A., & Morbidelli, A. (2014), Separating gas-giant and ice-giant planets by halting
1304 pebble accretion, *Astronomy and Astrophysics*, 572, A35, 10.1051/0004-6361/201423814.

1305

1306 Lammer, H. (1995), Mass loss of N 2 molecules from Triton by magnetospheric plasma interaction, *Planetary
1307 and Space Science*, 43, 845, 10.1016/0032-0633(94)00214-C.

1308

1309 Lamy, L., Prangé, R., Hansen, K. C., Clarke, J. T., Zarka, P., Cecconi, B., Aboudarham, J., André, N., Branduardi-
1310 Raymont, G., et al. (2012), Earth-based detection of Uranus' aurorae, *Geophysical Research Letters*, 39,
1311 L07105, 10.1029/2012GL051312.

1312

- 1313 Lamy, L., Prangé, R., Hansen, K. C., Tao, C., Cowley, S. W. H., Stallard, T. S., Melin, H., Achilleos, N., Guio, P.,
1314 et al. (2017), The aurorae of Uranus past equinox, *Journal of Geophysical Research (Space Physics)*, 122, 3997,
1315 10.1002/2017JA023918.
- 1316
- 1317 LeBeau, R. P., & Dowling, T. E. (1998), EPIC Simulations of Time-Dependent, Three-Dimensional Vortices with
1318 Application to Neptune's Great Dark SPOT, *Icarus*, 132, 239, 10.1006/icar.1998.5918.
- 1319
- 1320 Leconte, J., Selsis, F., Hersant, F., & Guillot, T. (2017), Condensation-inhibited convection in hydrogen-rich
1321 atmospheres . Stability against double-diffusive processes and thermal profiles for Jupiter, Saturn, Uranus,
1322 and Neptune, *Astronomy and Astrophysics*, 598, A98, 10.1051/0004-6361/201629140.
- 1323
- 1324 Lellouch, E., de Bergh, C., Sicardy, B., Ferron, S., & Käufl, H.-U. (2010), Detection of CO in Triton's atmosphere
1325 and the nature of surface-atmosphere interactions, *Astronomy and Astrophysics*, 512, L8, 10.1051/0004-
1326 6361/201014339.
- 1327
- 1328 Li, C., Le, T., Zhang, X., & Yung, Y. L. (2018), A high-performance atmospheric radiation package: With
1329 applications to the radiative energy budgets of giant planets, *Journal of Quantitative Spectroscopy and*
1330 *Radiative Transfer*, 217, 353, 10.1016/j.jqsrt.2018.06.002.
- 1331
- 1332 Lindal, G. F., Lyons, J. R., Sweetnam, D. N., Eshleman, V. R., Hinson, D. P., & Tyler, G. L. (1987), The atmosphere
1333 of Uranus: Results of radio occultation measurements with Voyager 2, *Journal of Geophysical Research*, 92,
1334 14987, 10.1029/JA092iA13p14987.
- 1335
- 1336 Lindal, G. F. (1992), The Atmosphere of Neptune: an Analysis of Radio Occultation Data Acquired with
1337 Voyager 2, *The Astronomical Journal*, 103, 967, 10.1086/116119.
- 1338

- 1339 Majeed, T., Waite, J.H., Bouger, S.W., Yelle, R.V., Gladstone, G.R., McConnell, J.C., Bhardwaj, A., (2006)
- 1340 The ionospheres–thermospheres of the giant planets, *Advances in Space Research*, 33, 197-211 (doi:
1341 10.1016/j.asr.2003.05.009)
- 1342
- 1343 Martin-Herrero, A., Romeo, I., & Ruiz, J. (2018), Heat flow in Triton: Implications for heat sources powering
1344 recent geologic activity, *Planetary and Space Science*, 160, 19, 10.1016/j.pss.2018.03.010.
- 1345
- 1346 Masters, A. (2018), A More Viscous-Like Solar Wind Interaction With All the Giant Planets, *Geophysical
1347 Research Letters*, 45, 7320, 10.1029/2018GL078416.
- 1348
- 1349 Masters, A. (2014), Magnetic reconnection at Uranus' magnetopause, *Journal of Geophysical Research
1350 (Space Physics)*, 119, 5520, 10.1002/2014JA020077.
- 1351
- 1352 Masters, A., Achilleos, N., Agnor, C. B., Campagnola, S., Charnoz, S., Christophe, B., Coates, A. J., Fletcher, L.
1353 N., Jones, G. H., et al. (2014), Neptune and Triton: Essential pieces of the Solar System puzzle, *Planetary and
1354 Space Science*, 104, 108, 10.1016/j.pss.2014.05.008.
- 1355
- 1356 Mauk, B. H., & Fox, N. J. (2010), Electron radiation belts of the solar system, *Journal of Geophysical Research
1357 (Space Physics)*, 115, A12220, 10.1029/2010JA015660.
- 1358
- 1359 McKinnon, W. B., Stern, S. A., Weaver, H. A., Nimmo, F., Bierson, C. J., Grundy, W. M., Cook, J. C., Cruikshank,
1360 D. P., Parker, A. H., et al. (2017), Origin of the Pluto-Charon system: Constraints from the New Horizons flyby,
1361 *Icarus*, 287, 2, 10.1016/j.icarus.2016.11.019.
- 1362
- 1363 McKinnon, W. B., & Leith, A. C. (1995), Gas drag and the orbital evolution of a captured Triton., *Icarus*, 118,
1364 392, 10.1006/icar.1995.1199.

- 1365
- 1366 McNutt, R. L., Selesnick, R. S., & Richardson, J. D. (1987), Low-energy plasma observations in the
1367 magnetosphere of Uranus, *Journal of Geophysical Research*, 92, 4399, 10.1029/JA092iA05p04399.
- 1368
- 1369 Mejnertsen, L., Eastwood, J. P., Chittenden, J. P., & Masters, A. (2016), Global MHD simulations of Neptune's
1370 magnetosphere, *Journal of Geophysical Research (Space Physics)*, 121, 7497, 10.1002/2015JA022272.
- 1371
- 1372 Melin, H., Stallard, T., Miller, S., Trafton, L. M., Encrenaz, T., & Geballe, T. R. (2011), Seasonal Variability in
1373 the Ionosphere of Uranus, *The Astrophysical Journal*, 729, 134, 10.1088/0004-637X/729/2/134.
- 1374
- 1375 Melin, H., Stallard, T. S., Miller, S., Geballe, T. R., Trafton, L. M., & O'Donoghue, J. (2013), Post-equinoctial
1376 observations of the ionosphere of Uranus, *Icarus*, 223, 741, 10.1016/j.icarus.2013.01.012.
- 1377
- 1378 Melin, H., Fletcher, L. N., Stallard, T. S., Miller, S., Trafton, L. M., Moore, L., O'Donoghue, J., Vervack, R. J.,
1379 Dello Russo, N., et al. (2019), The H₃⁺ ionosphere of Uranus: decades-long cooling and local-time
1380 morphology, *Philosophical Transactions of the Royal Society of London Series A*, 377, 20180408,
1381 10.1098/rsta.2018.0408.
- 1382
- 1383 Merrill, R. T., & McFadden, P. L. (1999), Geomagnetic polarity transitions, *Reviews of Geophysics*, 37, 201,
1384 10.1029/1998RG900004.
- 1385
- 1386 Millot, M., Coppari, F., Rygg, J. R., Correa Barrios, A., Hamel, S., Swift, D. C., & Eggert, J. H. (2019), Nanosecond
1387 X-ray diffraction of shock-compressed superionic water ice, *Nature*, 569, 251, 10.1038/s41586-019-1114-6.
- 1388
- 1389 Molter, E. M., de Pater, I., Roman, M. T., & Fletcher, L. N. (2019), Thermal Emission from the Uranian Ring
1390 System, *The Astronomical Journal*, 158, 47, 10.3847/1538-3881/ab258c.

- 1391
- 1392 Moreno, R., Marten, A., & Lellouch, E. (2009), Search for PH₃ in the Atmospheres of Uranus and Neptune at
1393 Millimeter Wavelength, AAS/Division for Planetary Sciences Meeting Abstracts #41, 28.02.,
- 1394
- 1395 Morley, C. V., Fortney, J. J., Marley, M. S., Visscher, C., Saumon, D., & Leggett, S. K. (2012), Neglected Clouds
1396 in T and Y Dwarf Atmospheres, *The Astrophysical Journal*, 756, 172, 10.1088/0004-637X/756/2/172.
- 1397
- 1398 Moses, J. I., & Poppe, A. R. (2017), Dust ablation on the giant planets: Consequences for stratospheric
1399 photochemistry, *Icarus*, 297, 33, 10.1016/j.icarus.2017.06.002.
- 1400
- 1401 Moses, J. I., Fletcher, L. N., Greathouse, T. K., Orton, G. S., & Hue, V. (2018), Seasonal stratospheric
1402 photochemistry on Uranus and Neptune, *Icarus*, 307, 124, 10.1016/j.icarus.2018.02.004.
- 1403
- 1404 Mousis, O., Atkinson, D. H., Cavalié, T., Fletcher, L. N., Amato, M. J., Aslam, S., Ferri, F., Renard, J.-B., Spilker,
1405 T., et al. (2018), Scientific rationale for Uranus and Neptune in situ explorations, *Planetary and Space Science*,
1406 155, 12, 10.1016/j.pss.2017.10.005.
- 1407
- 1408 Namouni, F., & Porco, C. (2002), The confinement of Neptune's ring arcs by the moon Galatea, *Nature*, 417,
1409 45, 10.1038/417045a.
- 1410
- 1411 Nettelmann, N., Helled, R., Fortney, J. J., & Redmer, R. (2013), New indication for a dichotomy in the interior
1412 structure of Uranus and Neptune from the application of modified shape and rotation data, *Planetary and
1413 Space Science*, 77, 143, 10.1016/j.pss.2012.06.019.
- 1414
- 1415 Neubauer, F. M. (1990), Satellite plasma interactions, *Advances in Space Research*, 10, 25, 10.1016/0273-
1416 1177(90)90083-C.

- 1417
- 1418 Nimmo, F., & Spencer, J. R. (2015), Powering Triton's recent geological activity by obliquity tides: Implications
1419 for Pluto geology, *Icarus*, 246, 2, 10.1016/j.icarus.2014.01.044.
- 1420
- 1421 Orton, G. S., Fletcher, L. N., Moses, J. I., Mainzer, A. K., Hines, D., Hammel, H. B., Martin-Torres, F. J., Burgdorf,
1422 M., Merlet, C., et al. (2014), Mid-infrared spectroscopy of Uranus from the Spitzer Infrared Spectrometer: 1.
1423 Determination of the mean temperature structure of the upper troposphere and stratosphere, *Icarus*, 243,
1424 494, 10.1016/j.icarus.2014.07.010.
- 1425
- 1426 Pearl, J. C., & Conrath, B. J. (1991), The albedo, effective temperature, and energy balance of Neptune, as
1427 determined from Voyager data, *Journal of Geophysical Research*, 96, 18921, 10.1029/91JA01087.
- 1428
- 1429 Pearl, J. C., Conrath, B. J., Hanel, R. A., Pirraglia, J. A., & Coustenis, A. (1990), The albedo, effective
1430 temperature, and energy balance of Uranus, as determined from Voyager IRIS data, *Icarus*, 84, 12,
1431 10.1016/0019-1035(90)90155-3.
- 1432
- 1433 Penny, M. T., Gaudi, B. S., Kerins, E., Rattenbury, N. J., Mao, S., Robin, A. C., & Calchi Novati, S. (2019),
1434 Predictions of the WFIRST Microlensing Survey. I. Bound Planet Detection Rates, *The Astrophysical Journal*
1435 Supplement Series, 241, 3, 10.3847/1538-4365/aafb69.
- 1436
- 1437 Petigura, E. A., Howard, A. W., Marcy, G. W., Johnson, J. A., Isaacson, H., Cargile, P. A., Hebb, L., Fulton, B. J.,
1438 Weiss, L. M., et al. (2017), The California-Kepler Survey. I. High-resolution Spectroscopy of 1305 Stars Hosting
1439 Kepler Transiting Planets, *The Astronomical Journal*, 154, 107, 10.3847/1538-3881/aa80de.
- 1440

- 1441 Plainaki, C., Lilensten, J., Radioti, A., Andriopoulou, M., Milillo, A., Nordheim, T. A., Dandouras, I., Coustenis,
1442 A., Grassi, D., et al. (2016), Planetary space weather: scientific aspects and future perspectives, *Journal of*
1443 *Space Weather and Space Climate*, 6, A31, 10.1051/swsc/2016024.
- 1444
- 1445 Plescia, J. B. (1987), Cratering history of the Uranian satellites: Umbriel, Titania, and Oberon, *Journal of*
1446 *Geophysical Research*, 92, 14918, 10.1029/JA092iA13p14918.
- 1447
- 1448 Plescia, J. B. (1987), Geological terrains and crater frequencies on Ariel, *Nature*, 327, 201, 10.1038/327201a0.
- 1449
- 1450 Podolak, M., & Helled, R. (2012), What Do We Really Know about Uranus and Neptune?, *The Astrophysical*
1451 *Journal*, 759, L32, 10.1088/2041-8205/759/2/L32.
- 1452
- 1453 Podolak, M., Helled, R., & Schubert, G. (2019), Effect of non-adiabatic thermal profiles on the inferred
1454 compositions of Uranus and Neptune, *Monthly Notices of the Royal Astronomical Society*, 487, 2653,
1455 10.1093/mnras/stz1467.
- 1456
- 1457 Pollack, J. B., Hubickyj, O., Bodenheimer, P., Lissauer, J. J., Podolak, M., & Greenzweig, Y. (1996), Formation
1458 of the Giant Planets by Concurrent Accretion of Solids and Gas, *Icarus*, 124, 62, 10.1006/icar.1996.0190.
- 1459
- 1460 Postberg, F., Kempf, S., Schmidt, J., Brilliantov, N., Beinsen, A., Abel, B., Buck, U., & Srama, R. (2009), Sodium
1461 salts in E-ring ice grains from an ocean below the surface of Enceladus, *Nature*, 459, 1098,
1462 10.1038/nature08046.
- 1463
- 1464 Prockter, L. M., Nimmo, F., & Pappalardo, R. T. (2005), A shear heating origin for ridges on Triton, *Geophysical*
1465 *Research Letters*, 32, L14202, 10.1029/2005GL022832.
- 1466

- 1467 Quirico, E., Douté, S., Schmitt, B., de Bergh, C., Cruikshank, D. P., Owen, T. C., Geballe, T. R., & Roush, T. L.
1468 (1999), Composition, Physical State, and Distribution of Ices at the Surface of Triton, *Icarus*, 139, 159,
1469 10.1006/icar.1999.6111.
- 1470
- 1471 Rages, K., Pollack, J. B., Tomasko, M. G., & Doose, L. R. (1991), Properties of scatterers in the troposphere
1472 and lower stratosphere of Uranus based on Voyager imaging data, *Icarus*, 89, 359, 10.1016/0019-
1473 1035(91)90183-T.
- 1474
- 1475 Redmer, R., Mattsson, T. R., Nettelmann, N., & French, M. (2011), The phase diagram of water and the
1476 magnetic fields of Uranus and Neptune, *Icarus*, 211, 798, 10.1016/j.icarus.2010.08.008.
- 1477
- 1478 Richardson, J. D., & McNutt, R. L. (1990), Low-energy plasma in Neptune's magnetosphere, *Geophysical*
1479 *Research Letters*, 17, 1689, 10.1029/GL017i010p01689.
- 1480
- 1481 Roman, M. T., Fletcher, L. N., Orton, G. S., Rowe-Gurney, N., & Irwin, P. G. J. (2019), Uranus in Northern Mid-
1482 Spring: Persistent Atmospheric Temperatures and Circulations Inferred from Thermal Imaging, *arXiv e-prints*,
1483 arXiv:1911.12830,.
- 1484
- 1485 Rymer, A., Mandt, K., Hurley, D., Lisse, C., Izenberg, N., Smith, H. T., Westlake, J., Bunce, E., Arridge, C., et al.
1486 (2019), Solar System Ice Giants: Exoplanets in our Backyard., *Bulletin of the American Astronomical Society*,
1487 51, 176,.
- 1488
- 1489 Sánchez-Lavega, A., Sromovsky, L. A., et al. (2018), Gas Giants. In: Galperin, B., Read, P.L., (eds) *Zonal Jets*
1490 *Phenomenology, Genesis and Physics*. Cambridge (doi: 10.1017/9781107358225).
- 1491

- 1492 Safronov, V. S. (1966), Sizes of the largest bodies falling onto the planets during their formation, Soviet
1493 Astronomy, 9, 987,.
- 1494
- 1495 Scarf, F. L., Gurnett, D. A., Kurth, W. S., & Poynter, R. L. (1987), Voyager 2 plasma wave observations at
1496 Uranus, Advances in Space Research, 7, 253, 10.1016/0273-1177(87)90226-2.
- 1497
- 1498 Selesnick, R. S. (1988), Magnetospheric convection in the nondipolar magnetic field of Uranus, Journal of
1499 Geophysical Research, 93, 9607, 10.1029/JA093iA09p09607.
- 1500
- 1501 Showalter, M. R., & Lissauer, J. J. (2006), The Second Ring-Moon System of Uranus: Discovery and Dynamics,
1502 Science, 311, 973, 10.1126/science.1122882.
- 1503
- 1504 Simon, A. A., Wong, M. H., & Hsu, A. I. (2019), Formation of a New Great Dark Spot on Neptune in 2018,
1505 Geophysical Research Letters, 46, 3108, 10.1029/2019GL081961.
- 1506
- 1507 Simon, A. A., Stern, S. A., & Hofstadter, M. (2018), Outer Solar System Exploration: A Compelling and Unified
1508 Dual Mission Decadal Strategy for Exploring Uranus, Neptune, Triton, Dwarf Planets, and Small KBOs and
1509 Centaurs, arXiv e-prints, arXiv:1807.08769,.
- 1510
- 1511 Simon, A. A., Rowe, J. F., Gaulme, P., Hammel, H. B., Casewell, S. L., Fortney, J. J., Gizis, J. E., Lissauer, J. J.,
1512 Morales-Juberias, R., et al. (2016), Neptune's Dynamic Atmosphere from Kepler K2 Observations:
1513 Implications for Brown Dwarf Light Curve Analyses, The Astrophysical Journal, 817, 162, 10.3847/0004-
1514 637X/817/2/162.
- 1515
- 1516 Slattery, W. L., Benz, W., & Cameron, A. G. W. (1992), Giant impacts on a primitive Uranus, Icarus, 99, 167,
1517 10.1016/0019-1035(92)90180-F.

1518

1519 Smith, B. A., Soderblom, L. A., Banfield, D., Barnet, C., Basilevksy, A. T., Beebe, R. F., Bollinger, K., Boyce, J.
1520 M., Brahic, A., et al. (1989), Voyager 2 at Neptune: Imaging Science Results, *Science*, 246, 1422,
1521 10.1126/science.246.4936.1422.

1522

1523 Smith, M. D., & Gierasch, P. J. (1995), Convection in the outer planet atmospheres including ortho-para
1524 hydrogen conversion., *Icarus*, 116, 159, 10.1006/icar.1995.1118.

1525

1526 Soderblom, L. A., Kieffer, S. W., Becker, T. L., Brown, R. H., Cook, A. F., Hansen, C. J., Johnson, T. V., Kirk, R. L.,
1527 & Shoemaker, E. M. (1990), Triton's Geyser-Like Plumes: Discovery and Basic Characterization, *Science*, 250,
1528 410, 10.1126/science.250.4979.410.

1529

1530 Soderlund, K. M., Heimpel, M. H., King, E. M., & Aurnou, J. M. (2013), Turbulent models of ice giant internal
1531 dynamics: Dynamos, heat transfer, and zonal flows, *Icarus*, 224, 97, 10.1016/j.icarus.2013.02.014.

1532

1533 Sromovsky, L. A., Karkoschka, E., Fry, P. M., Hammel, H. B., de Pater, I., & Rages, K. (2014), Methane depletion
1534 in both polar regions of Uranus inferred from HST/STIS and Keck/NIRC2 observations, *Icarus*, 238, 137,
1535 10.1016/j.icarus.2014.05.016.

1536

1537 Sromovsky, L. A., de Pater, I., Fry, P. M., Hammel, H. B., & Marcus, P. (2015), High S/N Keck and Gemini AO
1538 imaging of Uranus during 2012-2014: New cloud patterns, increasing activity, and improved wind
1539 measurements, *Icarus*, 258, 192, 10.1016/j.icarus.2015.05.029.

1540

1541 Stanley, S., & Bloxham, J. (2006), Numerical dynamo models of Uranus' and Neptune's magnetic fields, *Icarus*,
1542 184, 556, 10.1016/j.icarus.2006.05.005.

1543

- 1544 Stanley, S., & Bloxham, J. (2004), Convective-region geometry as the cause of Uranus' and Neptune's unusual
1545 magnetic fields, *Nature*, 428, 151, 10.1038/nature02376.
- 1546
- 1547 Stauffer, J., Marley, M. S., Gizis, J. E., Rebull, L., Carey, S. J., Krick, J., Ingalls, J. G., Lowrance, P., Glaccum, W.,
1548 et al. (2016), Spitzer Space Telescope Mid-IR Light Curves of Neptune, *The Astronomical Journal*, 152, 142,
1549 10.3847/0004-6256/152/5/142.
- 1550
- 1551 Stern, S. A., & McKinnon, W. B. (2000), Triton's Surface Age and Impactor Population Revisited in Light of
1552 Kuiper Belt Fluxes: Evidence for Small Kuiper Belt Objects and Recent Geological Activity, *The Astronomical
1553 Journal*, 119, 945, 10.1086/301207.
- 1554
- 1555 Stevenson, D. J. (1986), The Uranus-Neptune Dichotomy: the Role of Giant Impacts, *Lunar and Planetary
1556 Science Conference*, 1011,.
- 1557
- 1558 Stoker, C. R., & Toon, O. B. (1989), Moist convection on Neptune, *Geophysical Research Letters*, 16, 929,
1559 10.1029/GL016i008p00929.
- 1560
- 1561 Stone, E. C., Cooper, J. F., Cummings, A. C., McDonald, F. B., Trainor, J. H., Lal, N., McGuire, R., & Chenette,
1562 D. L. (1986), Energetic Charged Particles in the Uranian Magnetosphere, *Science*, 233, 93,
1563 10.1126/science.233.4759.93.
- 1564
- 1565 Stratman, P. W., Showman, A. P., Dowling, T. E., & Sromovsky, L. A. (2001), EPIC Simulations of Bright
1566 Companions to Neptune's Great Dark Spots, *Icarus*, 151, 275, 10.1006/icar.2001.6603.
- 1567
- 1568 Strobel, D. F., Cheng, A. F., Summers, M. E., & Strickland, D. J. (1990), Magnetospheric interaction with
1569 Triton's ionosphere, *Geophysical Research Letters*, 17, 1661, 10.1029/GL017i010p01661.

- 1570
- 1571 Stryk, T., & Stooke, P. J. (2008), Voyager 2 Images of Uranian Satellites: Reprocessing and New
1572 Interpretations, *Lunar and Planetary Science Conference*, 1362,.
- 1573
- 1574 Sun, Z.-P., Schubert, G., & Stoker, C. R. (1991), Thermal and humidity winds in outer planet atmospheres,
1575 *Icarus*, 91, 154, 10.1016/0019-1035(91)90134-F.
- 1576
- 1577 Tegler, S. C., Stufflebeam, T. D., Grundy, W. M., Hanley, J., Dustrud, S., Lindberg, G. E., Engle, A., Dillingham,
1578 T. R., Matthew, D., et al. (2019), A New Two-molecule Combination Band as a Diagnostic of Carbon Monoxide
1579 Diluted in Nitrogen Ice on Triton, *The Astronomical Journal*, 158, 17, 10.3847/1538-3881/ab199f.
- 1580
- 1581 Tegler, S. C., Grundy, W. M., Olkin, C. B., Young, L. A., Romanishin, W., Cornelison, D. M., &
1582 Khodadadkouchaki, R. (2012), Ice Mineralogy across and into the Surfaces of Pluto, Triton, and Eris, *The
1583 Astrophysical Journal*, 751, 76, 10.1088/0004-637X/751/1/76.
- 1584
- 1585 Thompson, W. R., & Sagan, C. (1990), Color and chemistry on Triton, *Science*, 250, 415,
1586 10.1126/science.11538073.
- 1587
- 1588 Tiscareno, M. S., Hedman, M. M., Burns, J. A., & Castillo-Rogez, J. (2013), Compositions and Origins of Outer
1589 Planet Systems: Insights from the Roche Critical Density, *The Astrophysical Journal*, 765, L28, 10.1088/2041-
1590 8205/765/2/L28.
- 1591
- 1592 Tittemore, W. C., & Wisdom, J. (1990), Tidal evolution of the Uranian satellites III. Evolution through the
1593 Miranda-Umbriel 3:1, Miranda-Ariel 5:3, and Ariel-Umbriel 2:1 mean-motion commensurabilities, *Icarus*, 85,
1594 394, 10.1016/0019-1035(90)90125-S.
- 1595

- 1596 Tosi, F., Turrini, D., Coradini, A., & Filacchione, G. (2010), Probing the origin of the dark material on Iapetus,
1597 Monthly Notices of the Royal Astronomical Society, 403, 1113, 10.1111/j.1365-2966.2010.16044.x.
- 1598
- 1599 Turrini, D., Politi, R., Peron, R., Grassi, D., Plainaki, C., Barbieri, M., Lucchesi, D. M., Magni, G., Altieri, F., et al.
1600 (2014), The comparative exploration of the ice giant planets with twin spacecraft: Unveiling the history of
1601 our Solar System, Planetary and Space Science, 104, 93, 10.1016/j.pss.2014.09.005.
- 1602
- 1603 Venturini, J., & Helled, R. (2017), The Formation of Mini-Neptunes, The Astrophysical Journal, 848, 95,
1604 10.3847/1538-4357/aa8cd0.
- 1605
- 1606 Waite, J. H., Perryman, R. S., Perry, M. E., Miller, K. E., Bell, J., Cravens, T. E., Glein, C. R., Grimes, J., Hedman,
1607 M., et al. (2018), Chemical interactions between Saturn's atmosphere and its rings, Science, 362, aat2382,
1608 10.1126/science.aat2382.
- 1609
- 1610 Wakeford, H. R., Visscher, C., Lewis, N. K., Kataria, T., Marley, M. S., Fortney, J. J., & Mandell, A. M. (2017),
1611 High-temperature condensate clouds in super-hot Jupiter atmospheres, Monthly Notices of the Royal
1612 Astronomical Society, 464, 4247, 10.1093/mnras/stw2639.
- 1613
- 1614 Wang, C., & Richardson, J. D. (2004), Interplanetary coronal mass ejections observed by Voyager 2 between
1615 1 and 30 AU, Journal of Geophysical Research (Space Physics), 109, A06104, 10.1029/2004JA010379.
- 1616
- 1617 Wei, Y., Pu, Z., Zong, Q., Wan, W., Ren, Z., Fraenz, M., Dubinin, E., Tian, F., Shi, Q., et al. (2014), Oxygen escape
1618 from the Earth during geomagnetic reversals: Implications to mass extinction, Earth and Planetary Science
1619 Letters, 394, 94, 10.1016/j.epsl.2014.03.018.
- 1620

- 1621 Witasse, O., Sánchez-Cano, B., Mays, M. L., Kajdič, P., Opgenoorth, H., Elliott, H. A., Richardson, I. G.,
1622 Zouganelis, I., Zender, J., et al. (2017), Interplanetary coronal mass ejection observed at STEREO-A, Mars,
1623 comet 67P/Churyumov-Gerasimenko, Saturn, and New Horizons en route to Pluto: Comparison of its Forbush
1624 decreases at 1.4, 3.1, and 9.9 AU, *Journal of Geophysical Research (Space Physics)*, 122, 7865,
1625 10.1002/2017JA023884.
- 1626
- 1627 Wong, M. H., Tollefson, J., Hsu, A. I., de Pater, I., Simon, A. A., Hueso, R., Sánchez-Lavega, A., Sromovsky, L.,
1628 Fry, P., et al. (2018), A New Dark Vortex on Neptune, *The Astronomical Journal*, 155, 117, 10.3847/1538-
1629 3881/aaa6d6.
- 1630
- 1631 Zarka, P., & Pedersen, B. M. (1986), Radio detection of uranian lightning by Voyager 2, *Nature*, 323, 605,
1632 10.1038/323605a0.
- 1633
- 1634 Zhang, Z., Hayes, A. G., Janssen, M. A., Nicholson, P. D., Cuzzi, J. N., de Pater, I., & Dunn, D. E. (2017), Exposure
1635 age of Saturn's A and B rings, and the Cassini Division as suggested by their non-icy material content, *Icarus*,
1636 294, 14, 10.1016/j.icarus.2017.04.008.
- 1637